Clustering aspects in nuclear structure and reaction

Yasuro Funaki (RIKEN)

9th APCTP-BLTP JINR Joint Workshop at Kazakhstan on ``Modern problems of nuclear and particle physics'' @Almaty Institute of Physics & Technology, June 28 - July 4, 2015.

Contents

- Brief introduction of ``Container'' picture for nuclear clustering
- Structures of excited states above the Hoyle state in ^{12}C
- Triple alpha reaction rate at low temperature via imaginary time theory

(Advertisement)

Motivation and background

THSR (Tohsaki-Horiuchi-Schuck-Röpke) wave function :
``Alpha condensate''-type w.f.

$$\Phi_{3\alpha}(B,b) = \mathcal{A}\left[\ \right]$$

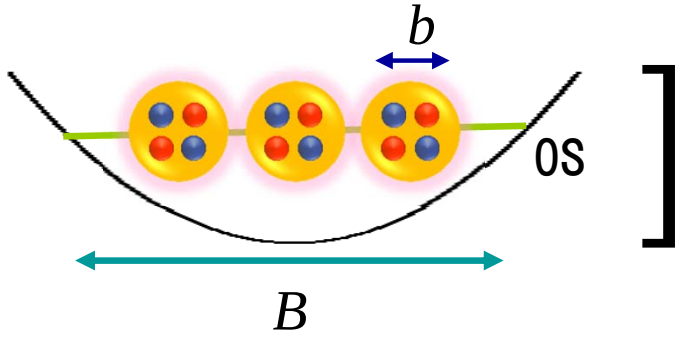

Motivation and background

THSR (Tohsaki-Horiuchi-Schuck-Röpke) wave function :
``Alpha condensate''-type w.f.

$$\Phi_{3\alpha}(B,b) = \mathcal{A}\left[\right]$$

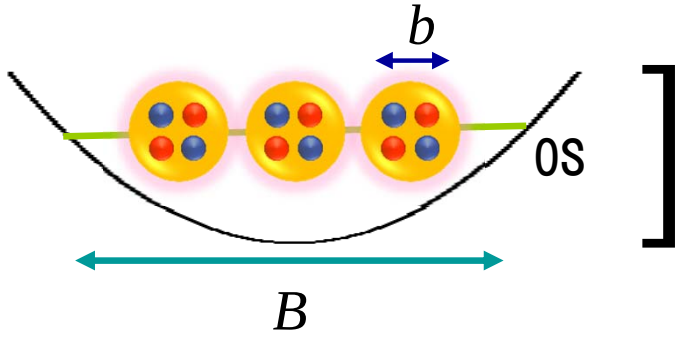

This, in general, gives ``container'' picture of nuclear clustering

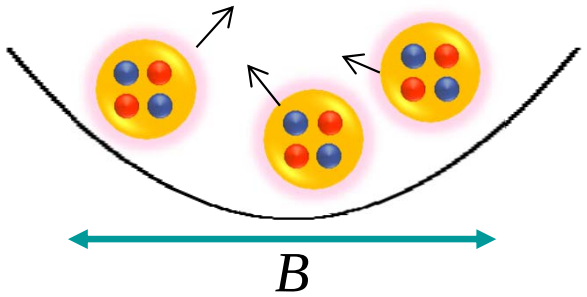

Nonlocalized clustering

Characterized by a size parameter B of the container, corresponding to nuclear size.

Motivation and background

THSR (Tohsaki-Horiuchi-Schuck-Röpke) wave function :
``Alpha condensate''-type w.f.

$$\Phi_{3\alpha}(B,b) = \mathcal{A}\left[\right]$$

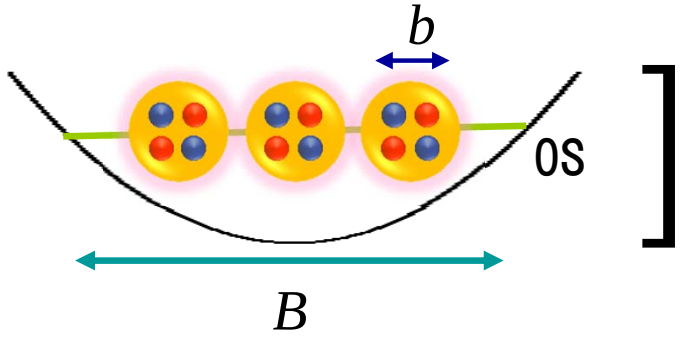

This, in general, gives ``container'' picture of nuclear clustering

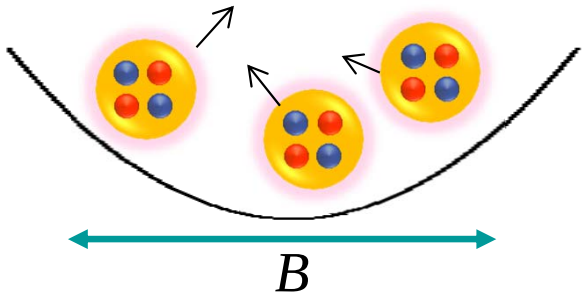

Nonlocalized clustering

Characterized by a size parameter *B* of the container, corresponding to nuclear size.

Quite different from conventional picture of clustering (Brink w.f.)

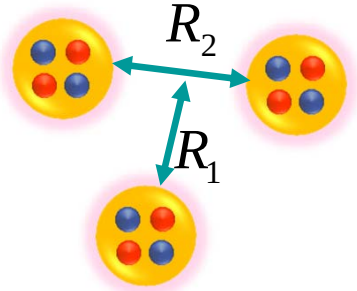

Localized clustering

Characterized by relative-distance parameters *R's between clusters.*

Motivation and background

This, in general, gives ``container'' picture of nuclear clustering

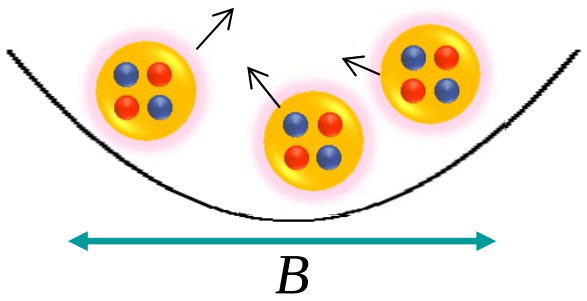

Nonlocalized clustering

Characterized by a size parameter *B* of the container, corresponding to nuclear size.

^{8}Be(0^{+}) *Y. F. et al., PTP108, 297(2002);*

^{12}C(0_{2}^{+}) *Y. F. et al., PRC67, 051306(R)(2003);PRC80, 064326(2009).*

^{20}Ne (^{16}O-α) *B. Zhou,Y. F. et al., PRC86, 014301 (2012); PRL 110, 262501(2013); PRC 89, 034319 (2014).*

3α and 4α linear chain states T. Suhara, Y. F. et al., PRL112, 062501 (2014)

^{9}Be (α- α-n) M. Lyu, Y. F. et al., PRC91, 014313(2015).

$^{9}_{\Lambda}$Be(0^{+}) Y. F. et al., PTEP 2014, 113D01

^{12}C(0_{1}^{+}) *Y. F. et al., PRC80, 064326(2009). B. Zhou, Y. F. et al., PTEP 2014, 101D01.*

Almost equivalent to the w.fs. obtained by the corresponding full cal. (RGM/GCM)

Providing basic understanding of the nuclear clustering

Y. F. H. Horiuchi, A. Tohsaki, PPNP82, 78-132 (2015).

Alpha condensate state

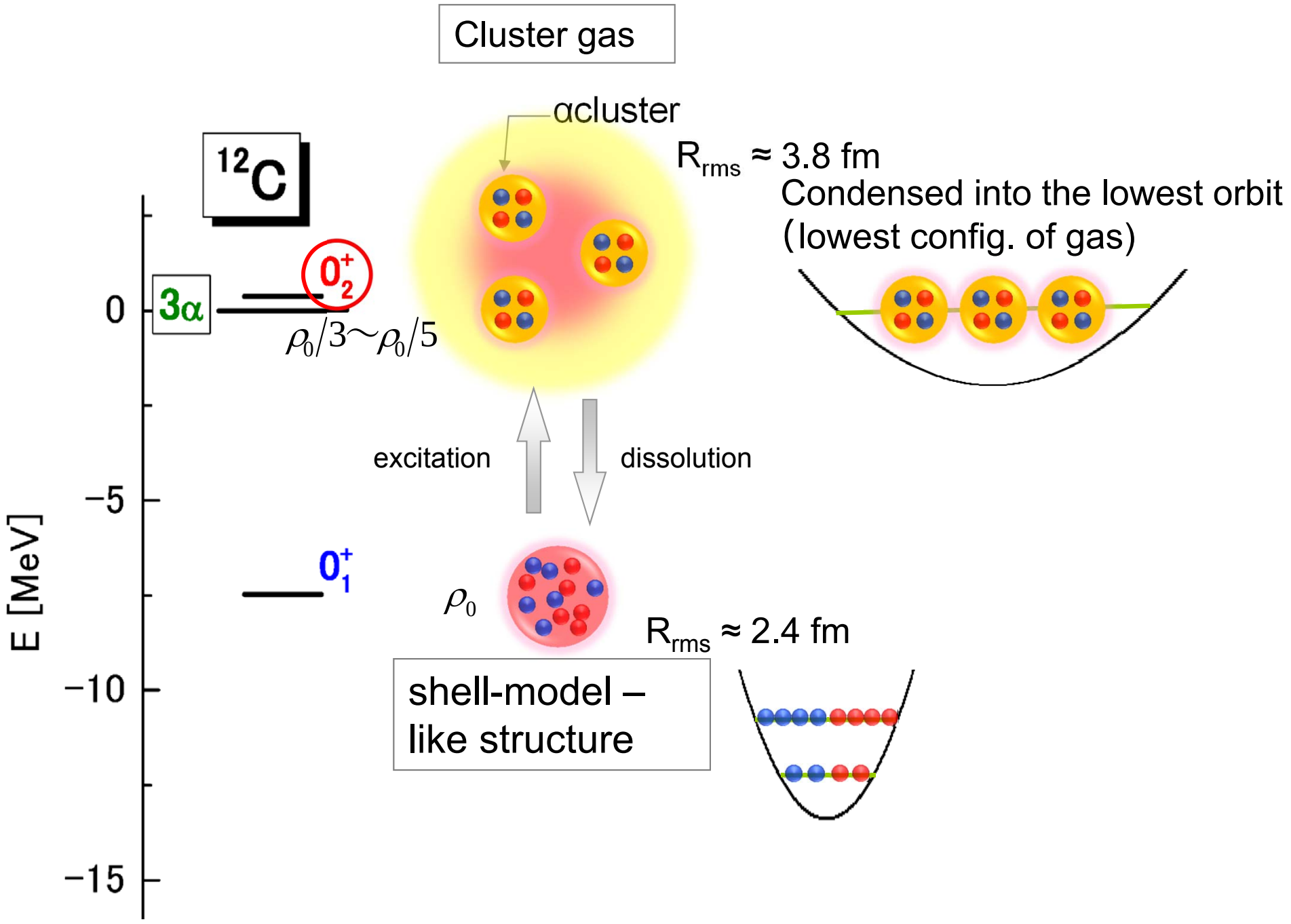

First example of alpha cond. state

Y. F. et al., PRC 67, 051306(2003)

Cluster gas

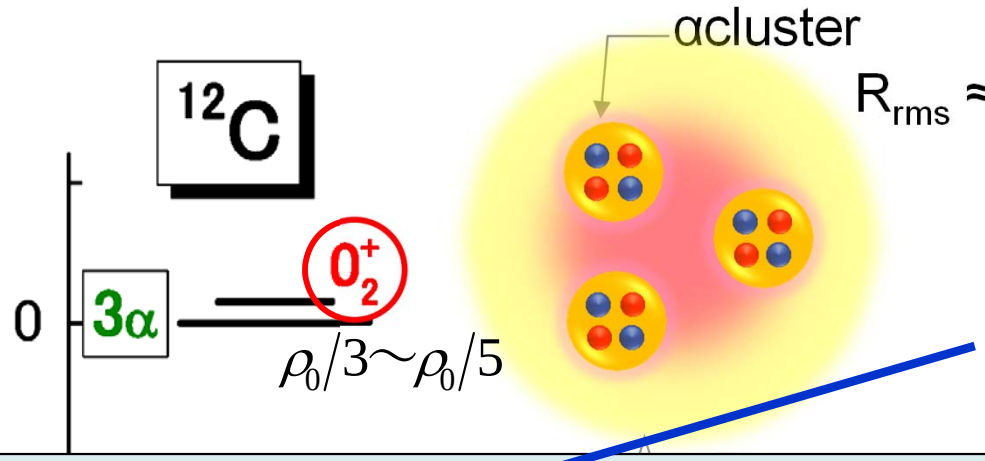

$R_{rms} \approx 3.8$ fm

Condensed into the lowest orbit

(lowest config. of gas)

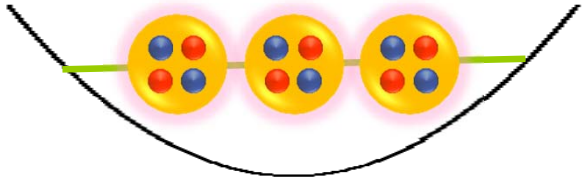

3α THSR w.f.

RGM

$$\left\langle \phi_{\alpha_1}\phi_{\alpha_2}\phi_{\alpha_3} \middle| H-E \middle| \mathcal{A}\left\{ \chi_{3\alpha}^{RGM}(\xi_1,\xi_2)\phi_{\alpha_1}\phi_{\alpha_2}\phi_{\alpha_3} \right\} \right\rangle = 0$$

$$\hat{\mathcal{P}}_{g.s.}\hat{\mathcal{P}}_{J=0}\mathcal{A}\left\{ \prod_{i=1}^{3} \chi_{3\alpha}^{THSR}(\boldsymbol{X}_i - \boldsymbol{X}_G : B_\perp, B_z)\phi_{\alpha_i} \right\} = \mathcal{A}\left\{ \chi_{3\alpha}^{RGM}(\xi_1,\xi_2)\phi_{\alpha_1}\phi_{\alpha_2}\phi_{\alpha_3} \right\}$$

$$\chi_{3\alpha}^{THSR}\left(\boldsymbol{X} : B_\perp, B_z\right) = e^{-\frac{2}{B_\perp^2}\left(X_x^2 + X_y^2\right) - \frac{2}{B_z^2}X_z^2}$$

($B_\perp$, B_z)=(7.6 fm, 2.5 fm) gives the very Hoyle state w.f.

This gives 99.3 % squared overlap with RGM w.f.

c.o.m. of *i*-th α particle

$$\boldsymbol{X}_i = \frac{\boldsymbol{r}_{4i-3} + \cdots + \boldsymbol{r}_{4i}}{4}$$

Total c.o.m.

$$\boldsymbol{X}_G = \frac{\boldsymbol{r}_1 + \cdots + \boldsymbol{r}_{4n}}{4n}$$

Comparison with exp. data for the Hoyle state (THSR w.f.)

Inelastic electron scattering ($0_1^+ \rightarrow 0_2^+$)

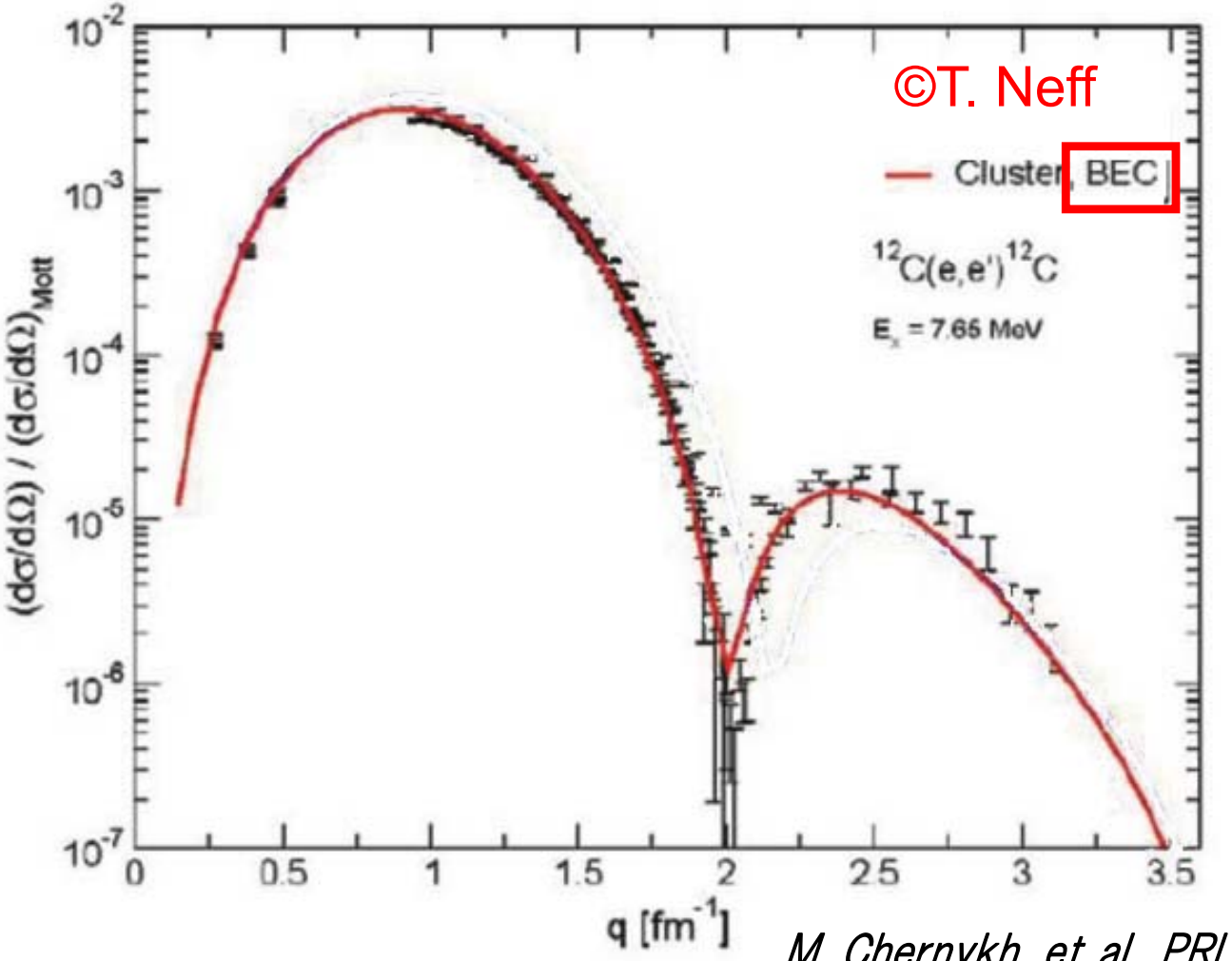

M. Chernykh. et al., PRL 98, 032501 (2007)

Energy (MeV)

$$E_{\rm cal} - E_{3\alpha}^{th} = 0.38$$
$$E_{\rm exp} - E_{3\alpha}^{th} = 0.23$$

α-decay width (MeV)

$$\Gamma_{\rm cal} = 7.7 \times 10^{-6}$$
$$\Gamma_{\rm exp} = 8.5(10) \times 10^{-6}$$

Monopole M.E. (fm^2)

$M(E0;\ 0_2^+ \rightarrow 0_1^+) = 6.4$ (Exp: 5.4(2))

B(E2) (e^{2}fm^4)

$B(E2;\ 2_1^+ \rightarrow 0_2^+) = 2.4$ (Exp: 0.73(13))

Very nicely reproduced by THSR w.f. (BEC-type)

0^+ states and rotational states in ^{12}C

Broad 0^+ state at10.3 MeV

- AMD: linear-chain-like: (0_4^+)
- OCM+CSM: family of αcond. (0_3^+) + linear-chain-like (0_4^+)
- Kamimura CSM: exactly confirmed two states (0_3^+, 0_4^+)
- Ali-Bodmer 3α by Ishikawa: monopole strength func. 0_3^+, 0_4^+
- Two 0^+ states

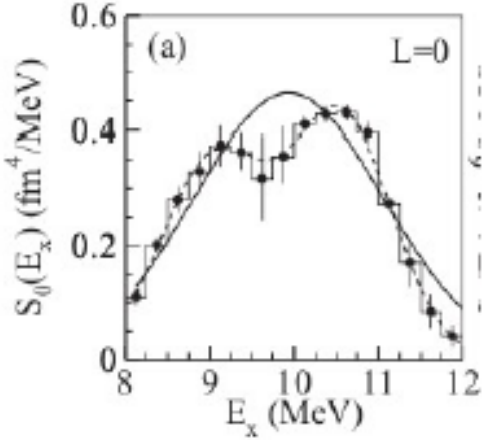

Result of MDA

Ex=9.04±0.09 MeV
Γ =1.45±0.18 MeV

Ex=10.56±0.06 MeV
Γ = 1.42±0.08 MeV

M. Itoh al., PRC 84, 054308 (2011).

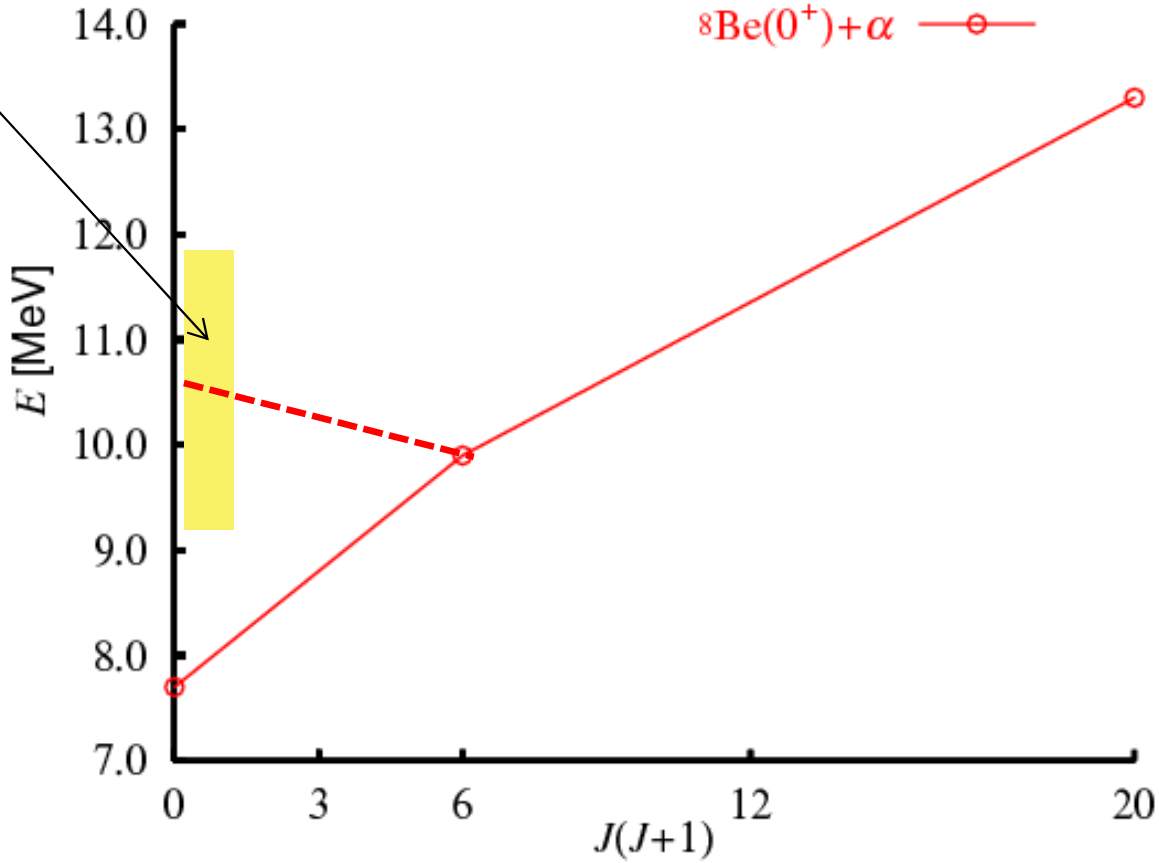

4^+ : *M. Freer et al., PRC 83, 034314 (2011)*

2^+ : *M. Itoh et al., NPA 738, 268 (2004)*

M. Freer et al., PRC 80, 041303 (2009)

W. R. Zimerman et al., PRC 84, 027304 (2011)

Deformed extended THSR (based on container picture), applied to ^{12}C

$$B_k^2 = b^2 + 2\beta_k^2 \quad (k = x, y, z)$$

$$\Phi_J^{\mathrm{THSR}}(B_x, B_y, B_z) = \mathcal{A}\left\{\prod_{i=1}^{3} \hat{\mathcal{P}}_J \chi^{\mathrm{THSR}}(B_x, B_y, B_z : \boldsymbol{X}_i - \boldsymbol{X}_G)\phi(\alpha_i)\right\}$$

c.o.m. of *i*-th α particle Total c.o.m.

$$\chi^{\mathrm{THSR}}(B_x, B_y, B_z : \boldsymbol{X} - \boldsymbol{X}_G) = \exp\left(-\sum_k^{x,y,z}\left\{\frac{2}{B_k^2}(X_k - X_{Gk})^2\right\}\right)$$

$$= \exp\left(-\sum_k^{x,y,z}\left\{\frac{1}{B_k^2}\xi_{1k}^2 + \frac{4}{3B_k^2}\xi_{2k}^2\right\}\right)$$

$$\chi_{new}^{\mathrm{THSR}} = \exp\left(-\sum_k^{x,y,z}\left\{\frac{1}{(B_k^{(1)})^2}\xi_{1k}^2 + \frac{4}{3(B_k^{(2)})^2}\xi_{2k}^2\right\}\right)$$

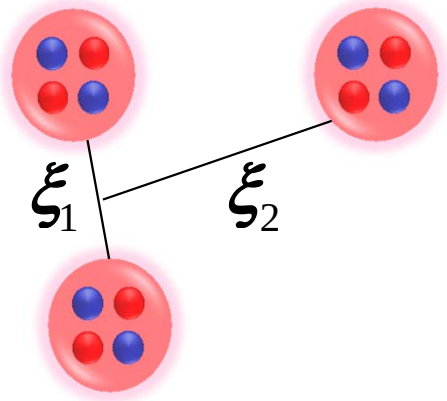

Alpha can occupy different orbit.

^{8}Be + alpha correlation can be taken into account.

For the g.s. B. Zhou , Y. F. et al., PTEP 2011,101D01.

The way of calculating energy spectra using ext.-THSR w.f.

$$B_k^2 = b^2 + 2\beta_k^2 \ (k = x, y, z)$$
$$\beta_\perp \equiv \beta_x = \beta_y$$

Ext. THSR w.f.

$$\Phi_J^{\mathrm{THSR}}(B_\perp^{(1)}, B_z^{(1)}, B_\perp^{(2)}, B_z^{(2)}) = \mathcal{A}\left\{\prod_{i=1}^{3} \hat{\mathcal{P}}_J \chi^{\mathrm{THSR}}(B_\perp^{(1)}, B_z^{(1)}, B_\perp^{(2)}, B_z^{(2)} : \boldsymbol{X_i} - \boldsymbol{X}_G)\phi(\alpha_i)\right\}$$

Hamiltonian (NN force: Volkov No.2 force)

$$H = \sum_{i=1}^{12} T_i - T_G + V^{(NN)} + V^{(C)}$$

Hill-Wheeler eq.

$$\sum_{\beta_\perp'^{(1)}, \beta_z'^{(1)}, \beta_\perp'^{(2)}, \beta_z'^{(2)}} \left\langle \Phi_J\left(\beta_\perp^{(1)}, \beta_z^{(1)}, \beta_\perp^{(2)}, \beta_z^{(2)}\right) \middle| \left(H - E_\lambda\right) \middle| \Phi_J\left(\beta_\perp'^{(1)}, \beta_z'^{(1)}, \beta_\perp'^{(2)}, \beta_z'^{(2)}\right) \right\rangle f_\lambda\left(\beta_\perp'^{(1)}, \beta_z'^{(1)}, \beta_\perp'^{(2)}, \beta_z'^{(2)}\right) = 0$$

Spurious continuum components are effectively eliminated by r^2 constraint method.

See Y. F. et al., PTP **115,** 115 (2006).

Energy Spectra (in parentheses: rms radii)

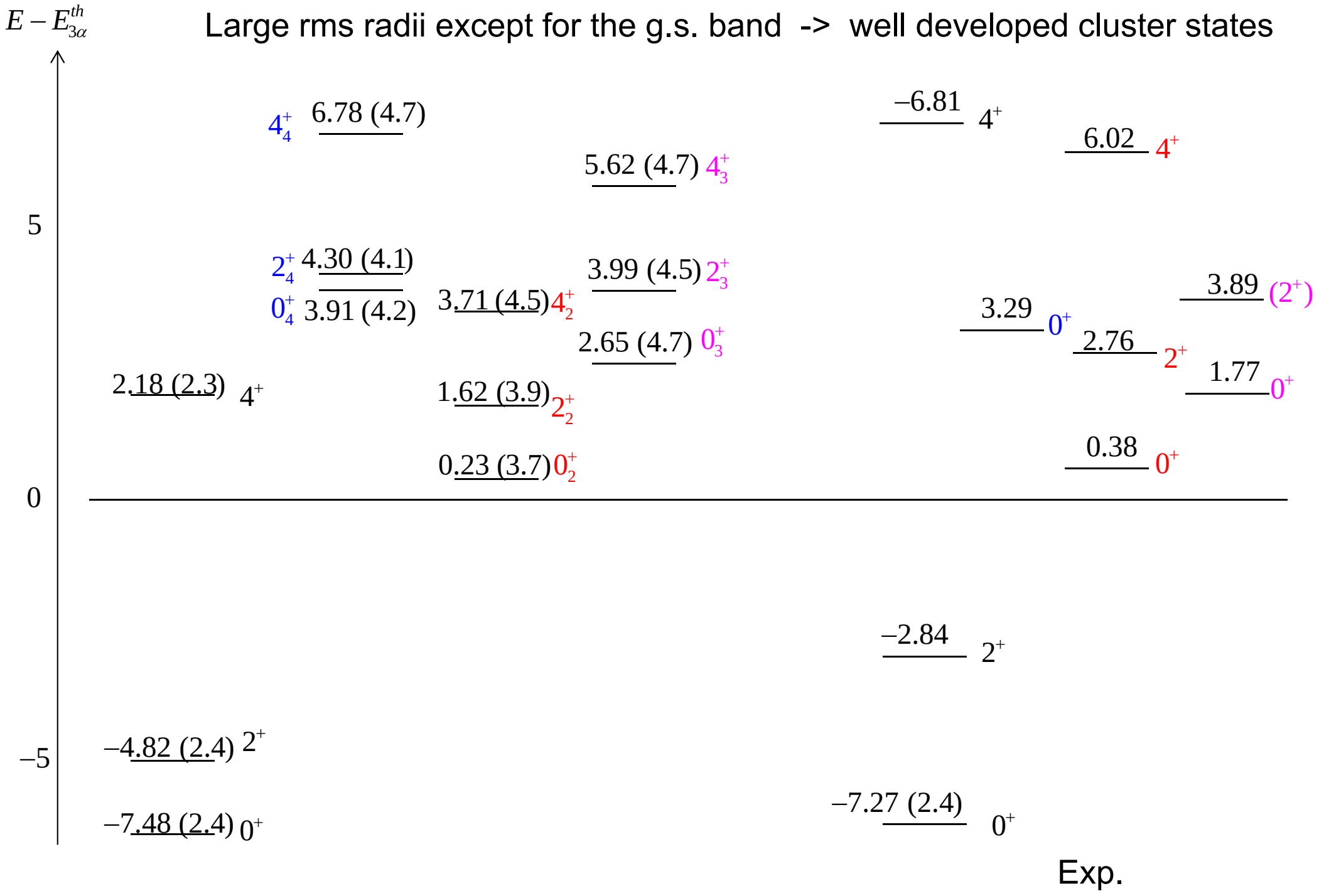

Energy Spectra (in parentheses: rms radii)

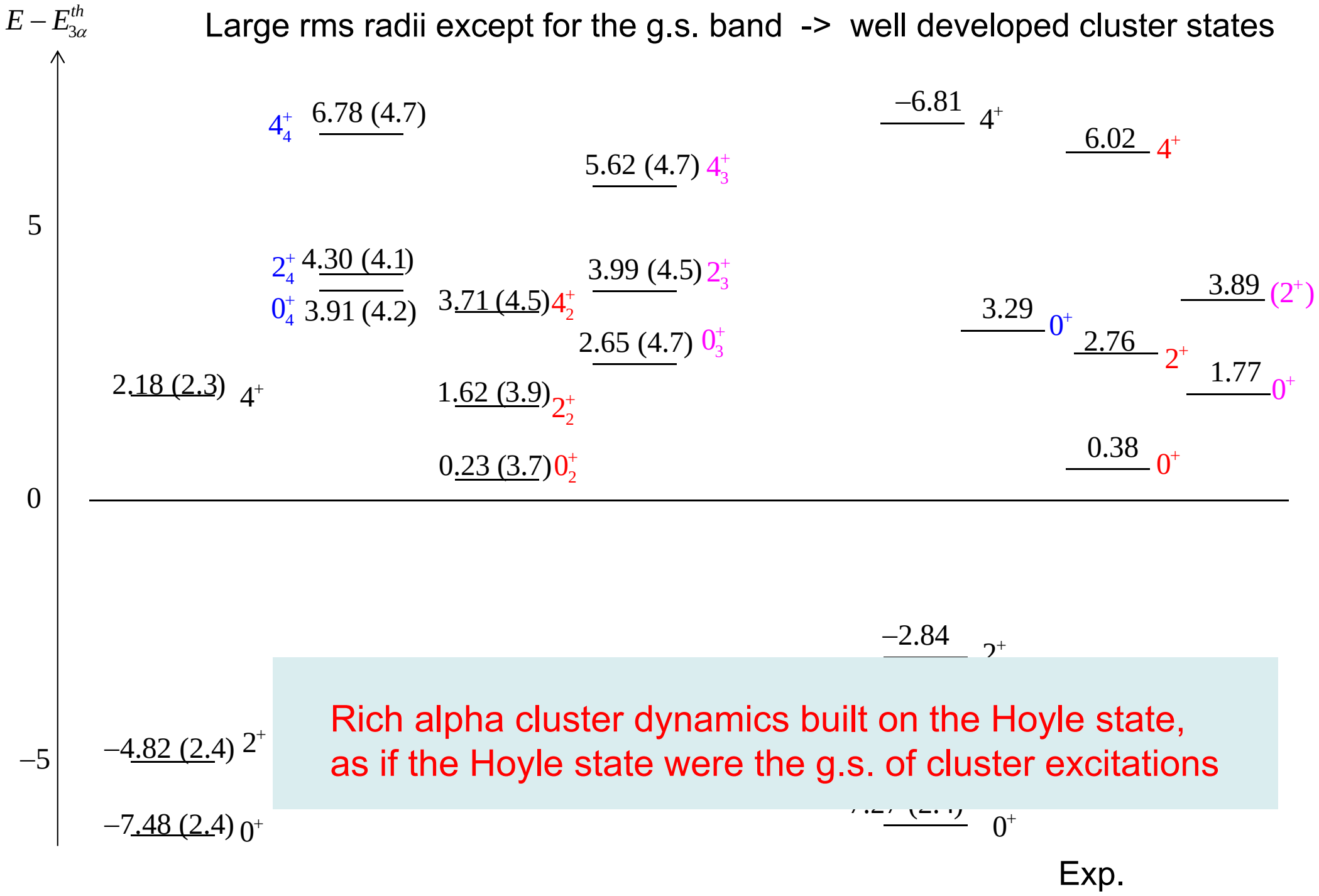

Definition of reduced width amplitude (RWA)

$$\mathcal{Y}_{[I,l]_J}(r) = \sqrt{\frac{12!}{4!8!}} \left\langle \left[\Psi_{^8\mathrm{Be}}(I), Y_l(\hat{\xi}) \right]_{JM} \frac{\delta(\xi - r)}{\xi^2} \phi_\alpha \middle| \Psi_{^{12}\mathrm{C}}(JM) \right\rangle$$

Overlap amplitude between ^{8}Be+alpha and ^{12}C

Definition of S-factor

$$S^2_{[I,l]_J} = \int dr \left(r \times \mathcal{Y}_{[I,l]_J}(r) \right)^2$$

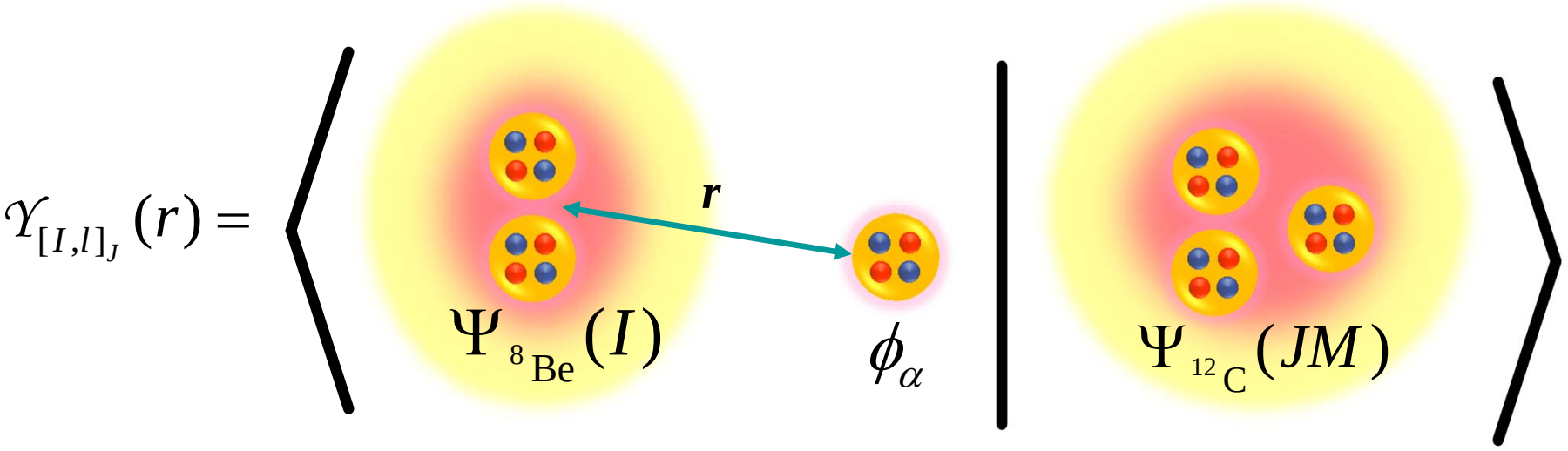

S-factor

$E - E^{th}_{3\alpha}$

5

0

−5

4^+_4

2^+_4

0^+_4

4^+_2

2^+_2

0^+_2

4^+_3

2^+_3

0^+_3

$[^8Be(I),\alpha(l)]_J$

Largest contributions from [0,J] channel

-> ^8Be + α rotation

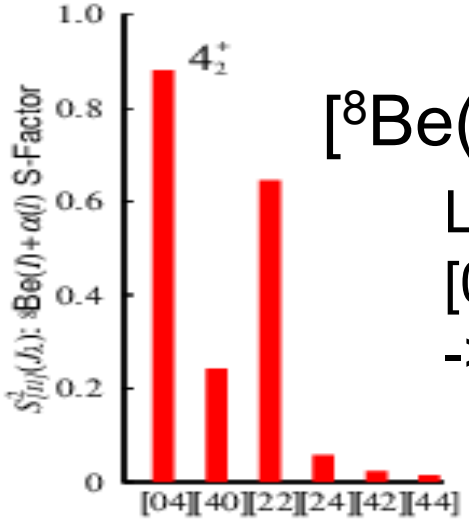

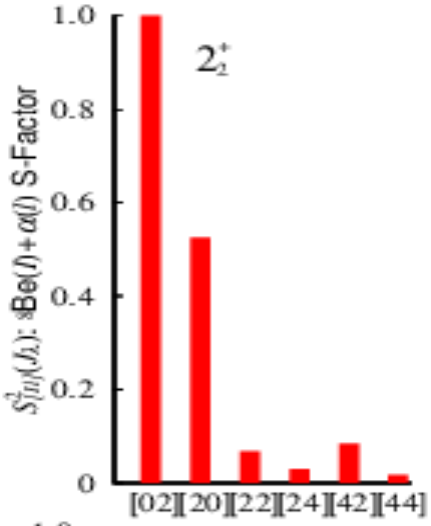

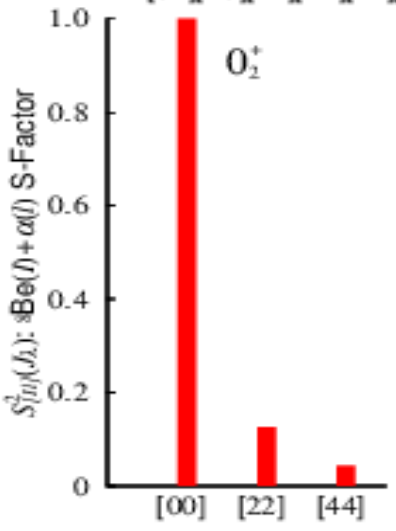

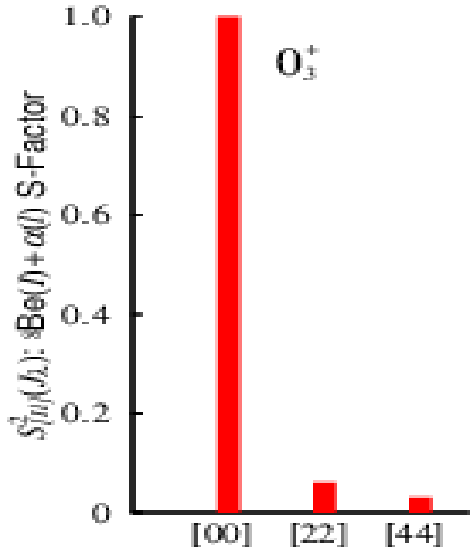

Rotational structure of the Hoyle band

Y. F. arXiv: 1408.5855 (submitted to PRC(R))

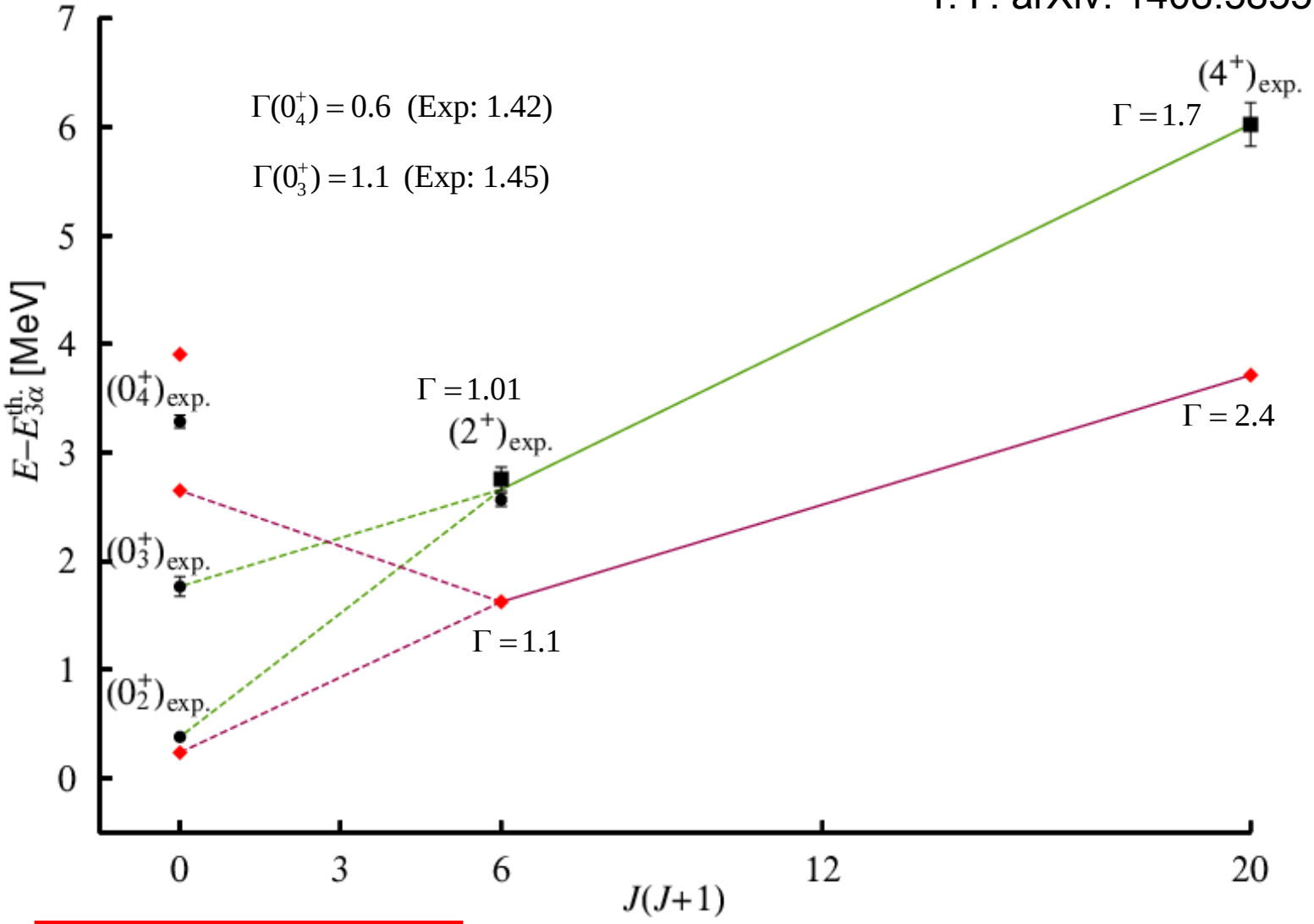

$B(E2;\ 4_2^+ \to 2_2^+) = 591$

$B(E2;\ 2_2^+ \to 0_2^+) = 295$

$B(E2;\ 2_2^+ \to 0_3^+) = 104$

$B(E2;\ 2_2^+ \to 0_4^+) = 27$

Fragmented into the Hoyle state and 0_3^+ state

The Hoyle state is not a simple bandhead of α+^{8}Be rotation

Specificity of the Hoyle state as the 3-alpha condensate

α rotates outside the core -> α rotates inside the core (α cond.)

Rotational structure of the Hoyle band

Y. F. arXiv: 1408.5855 (submitted to PRC(R))

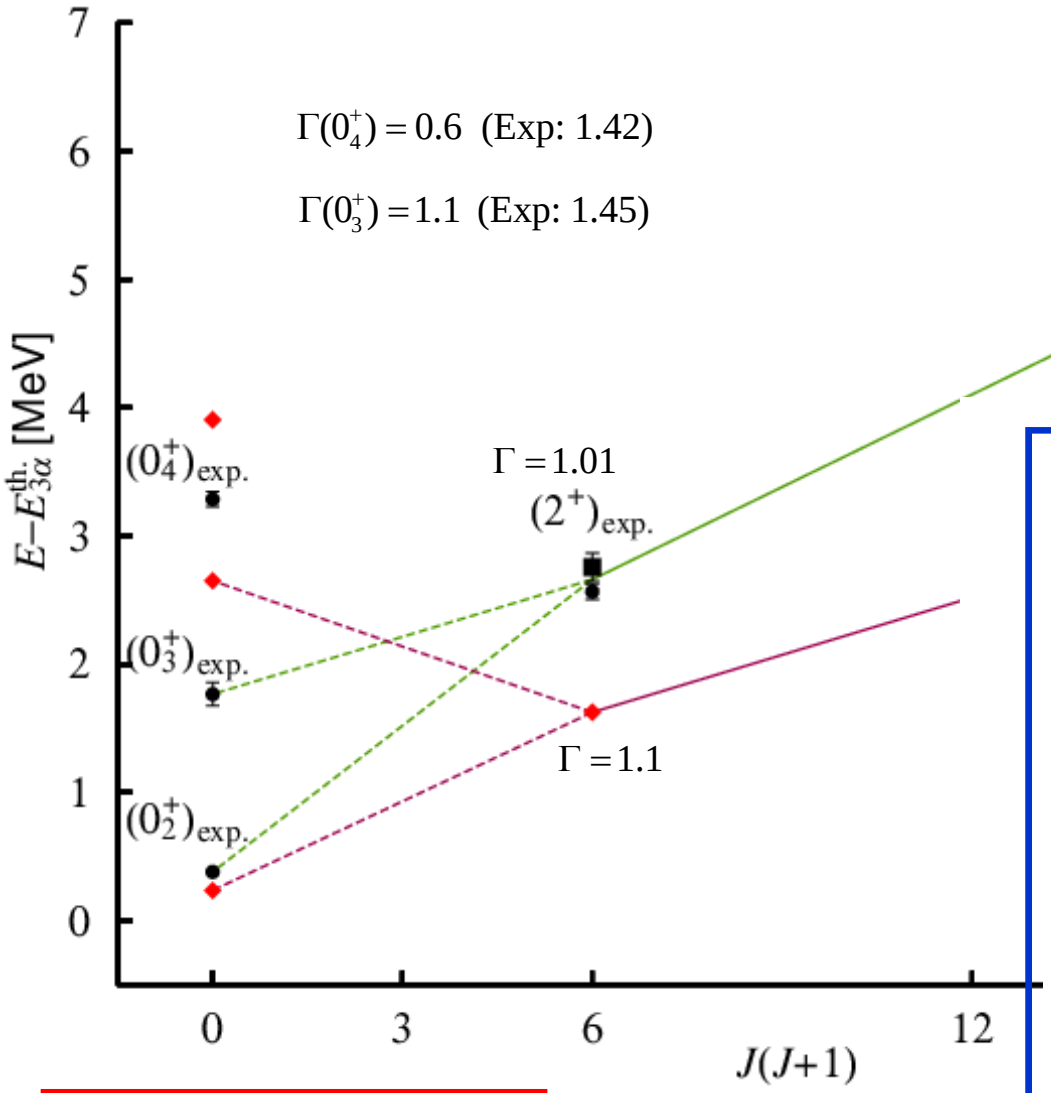

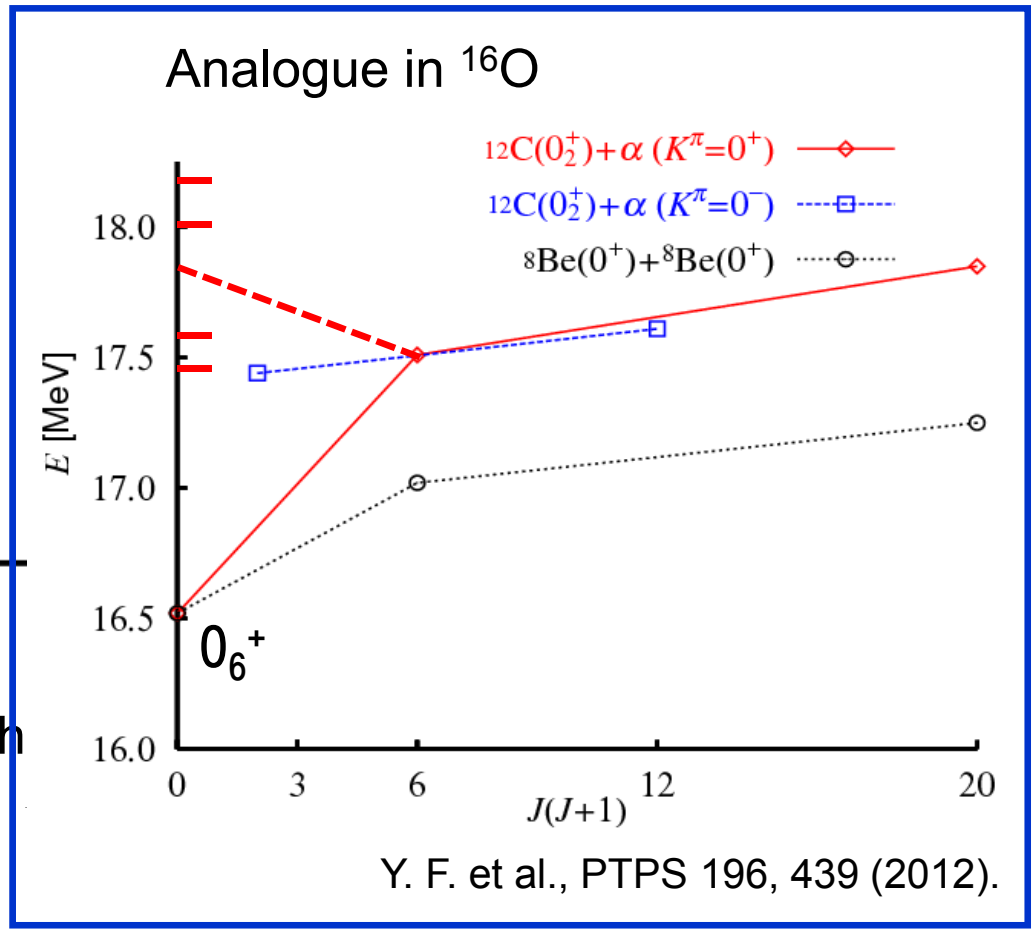

Y. F. et al., PTPS 196, 439 (2012).

$B(E2;\ 4_2^+ \to 2_2^+) = 591$

$B(E2;\ 2_2^+ \to 0_2^+) = 295$

$B(E2;\ 2_2^+ \to 0_3^+) = 104$

$B(E2;\ 2_2^+ \to 0_4^+) = 27$

Fragmented into th

The Hoyle state i

Specificity of t

α rotates outside the core -> α rotates inside the core (α cond.)

0_3^+ state: higher nodal excitation of the Hoyle state

RWAs of the 0_1^+ , 0_2^+ , 0_3^+ states for ^{8}Be(0+)+α(S) channel

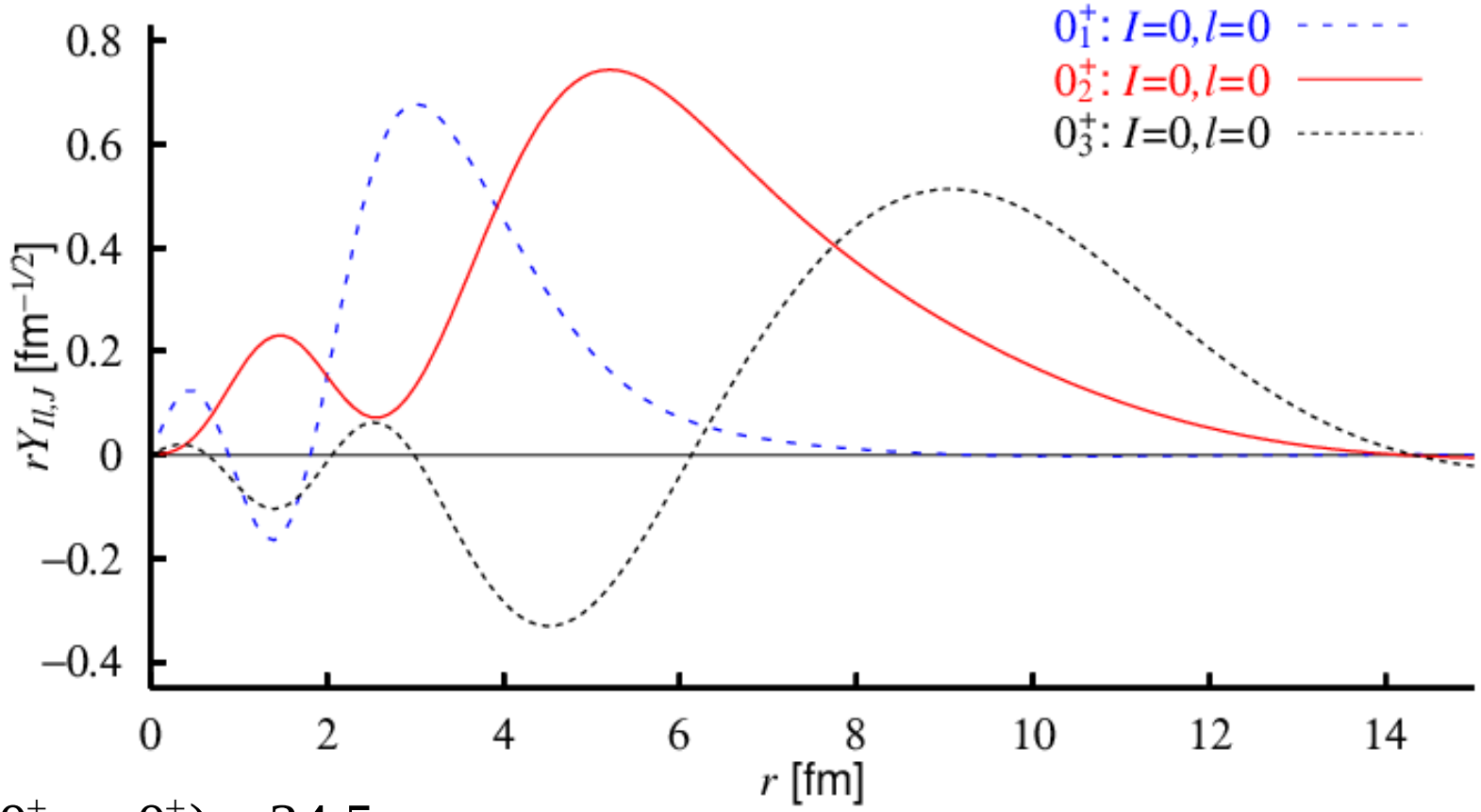

$$M(E0;\ 0_3^+ \rightarrow 0_2^+) = 34.5$$

Very large monopole transition strength between the 0_2^+ and 0_3^+ states c.f. $M(E0;\ 0_2^+ \rightarrow 0_1^+) = 6.4$

0_1^+ state: 2 nodes

0_2^+ state: 3 nodal oscillation (nodes disappear due to the dissolution of ^{8}Be core)

0_3^+ state: 4 nodes (higher nodal structure)

S-factor

$[^8\mathrm{Be}(I),\alpha(l)]_J$

Largest contributions from [0,J] channel
-> ^{8}Be+α rotation

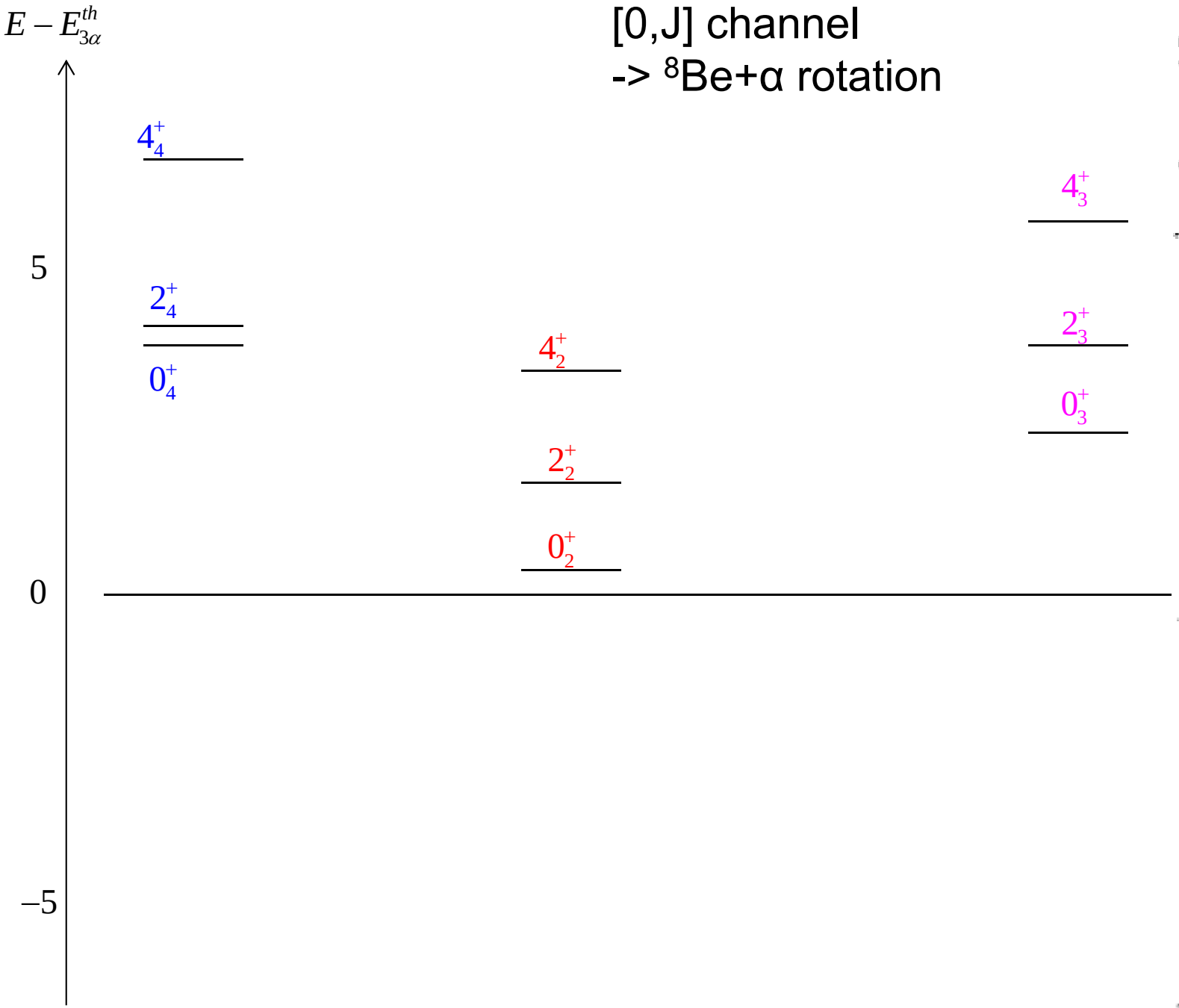

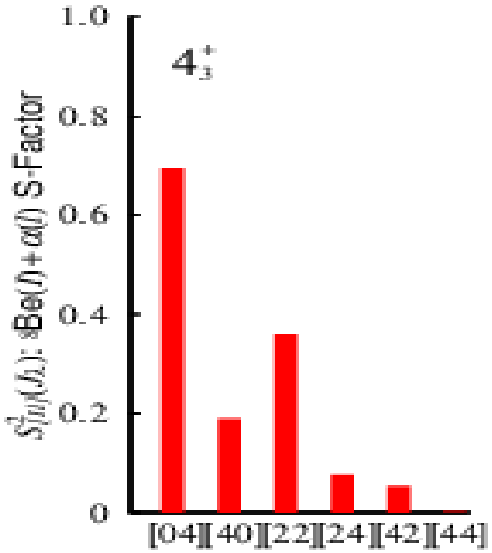

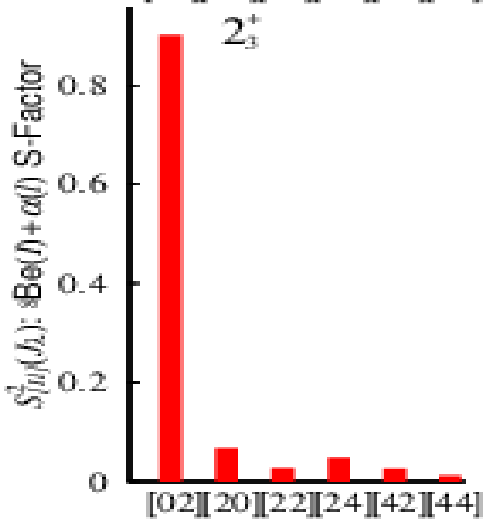

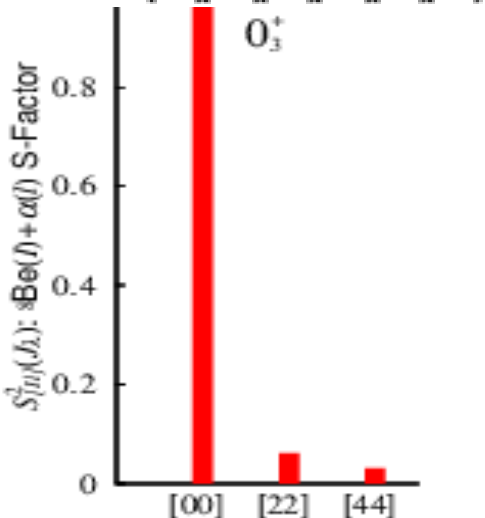

RWA of 0_3^+ , 2_3^+ , 4_3^+ states: ^{8}Be(0^+) + alpha(l) rotational band

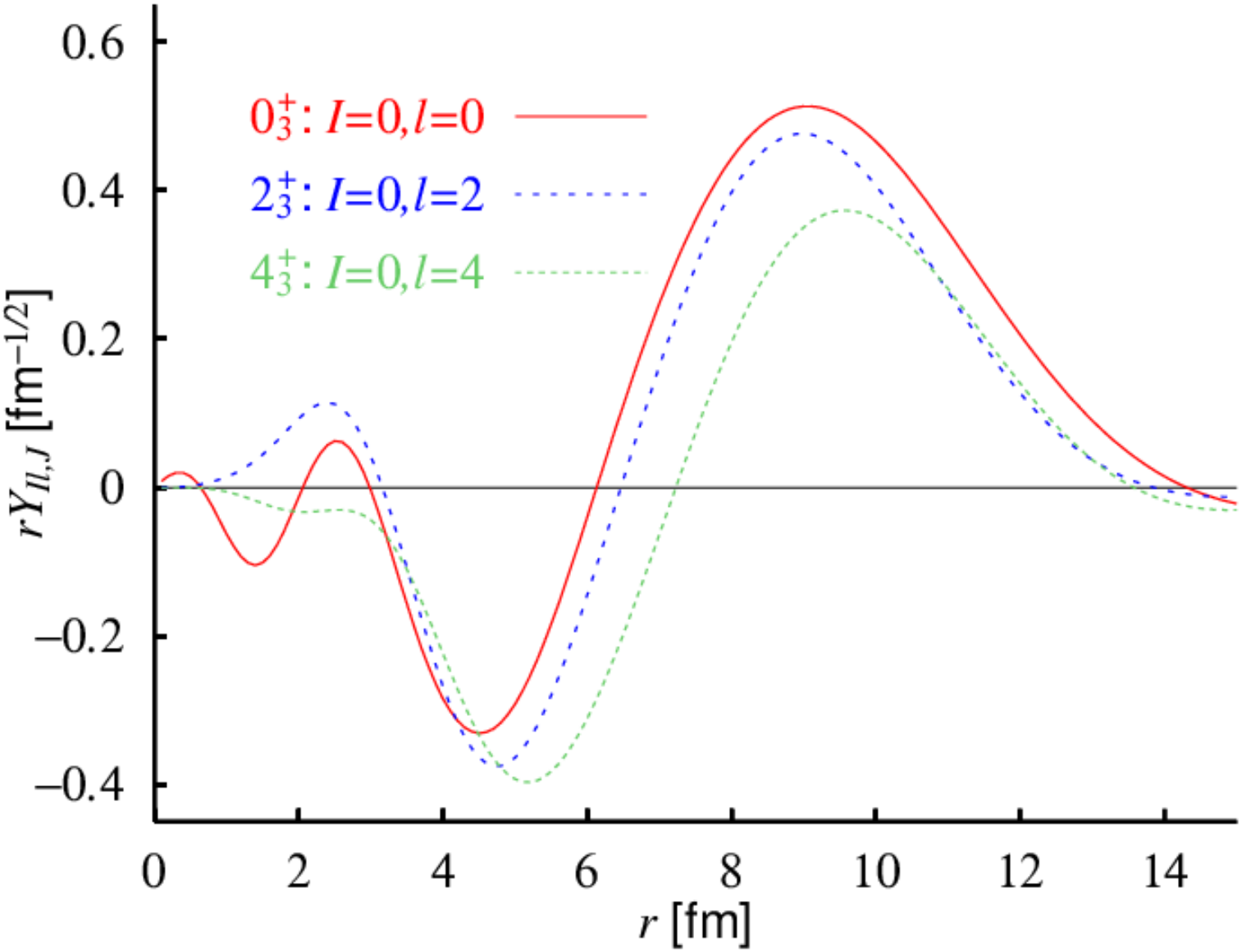

^{8}Be + alpha : well developed, constructed on the Hoyle state

0_3^+ : higher nodal behavior (4S)

S-factor

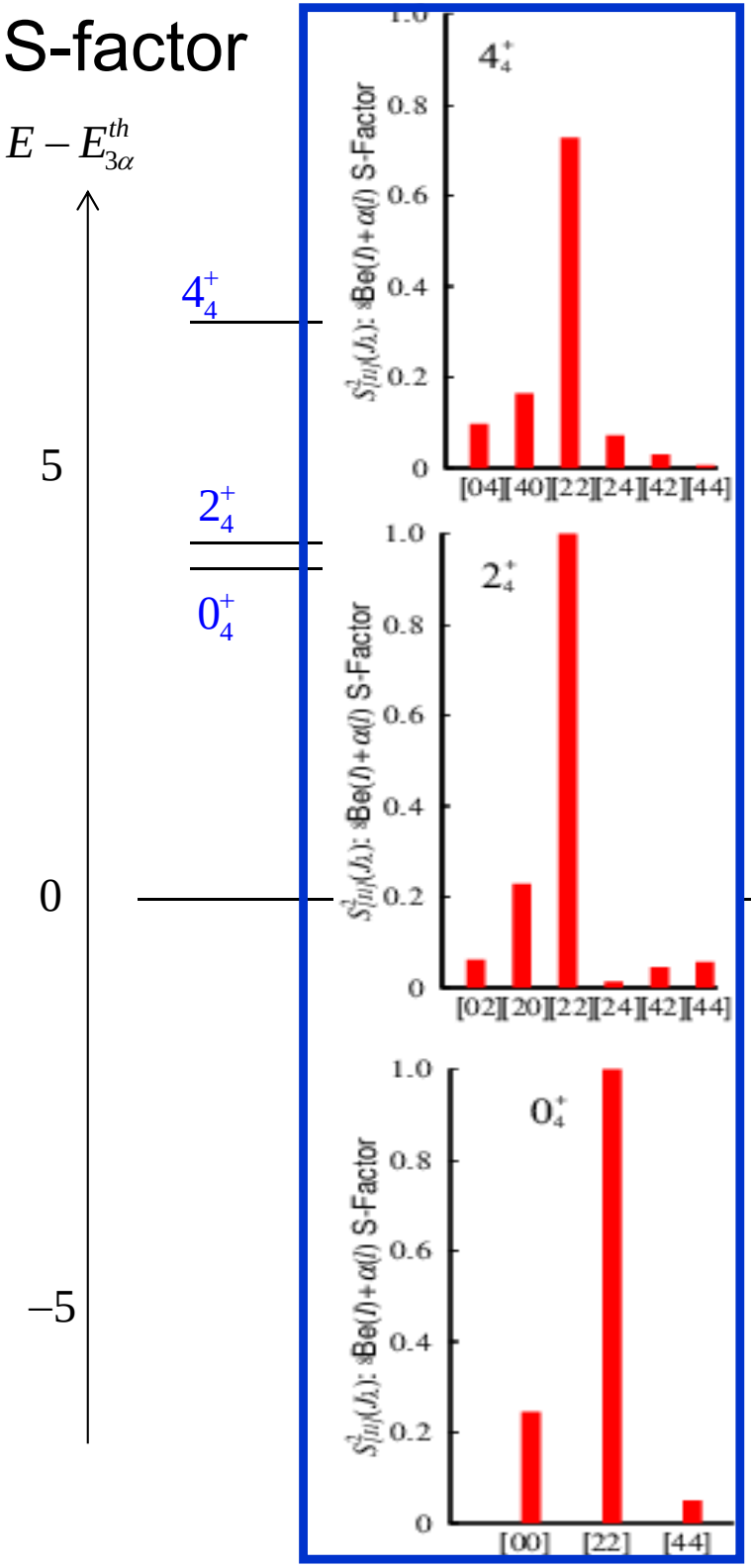

Large components from
[2,2] channel
-> corresponding to vibrational mode ?

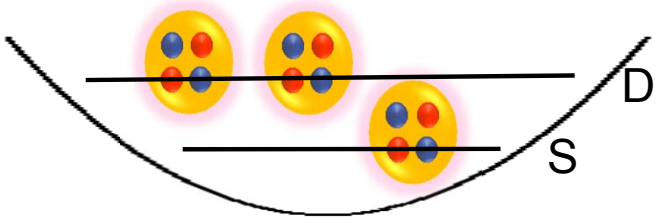

Two α's jump into D-orbit, coupling to J=0,2,4 ?

Possible interpretations of these bands

Y. F. in preparation

Rich alpha cluster dynamics built on the Hoyle state,
as if the Hoyle state were the g.s. of cluster excitations

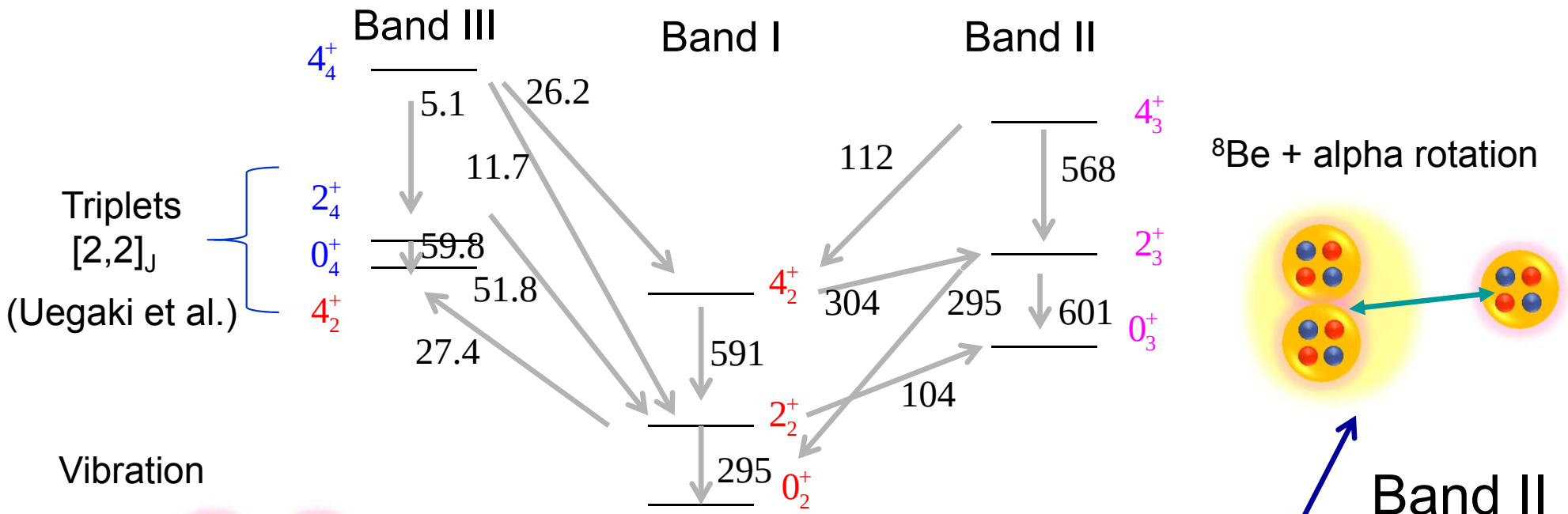

Vibration

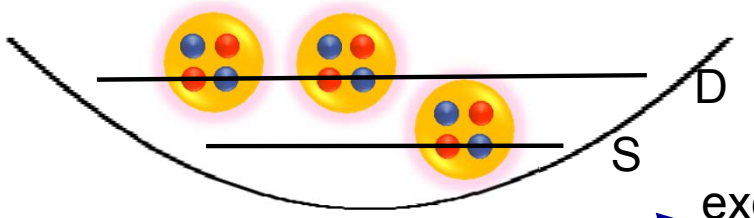

Band II

excited

Band II

excited

0_2^+: condensate

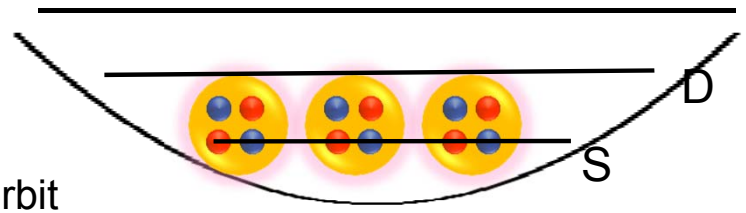

^{8}Be + alpha

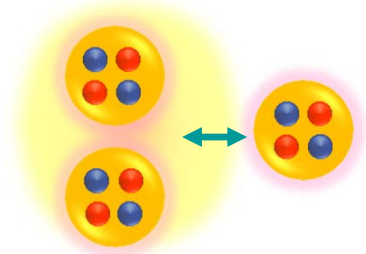

Vibrational picture:

0_2^+ : 3alphas sit in S-orbit
2_2^+ : one alpha jumps into D-orbit
4_2^+ : one alpha jumps into G-orbit
(+ 2 alphas jump into D-orbit)

Band I

Mixture between
^{8}Be + alpha rotation and vibration ?

Triple-alpha thermonuclear reaction rate

co-worked with T. Akahori (Hitachi) and K.Yabana (U. Tsukuba)

Dominant ^{12}C synthesis process depends on temperature

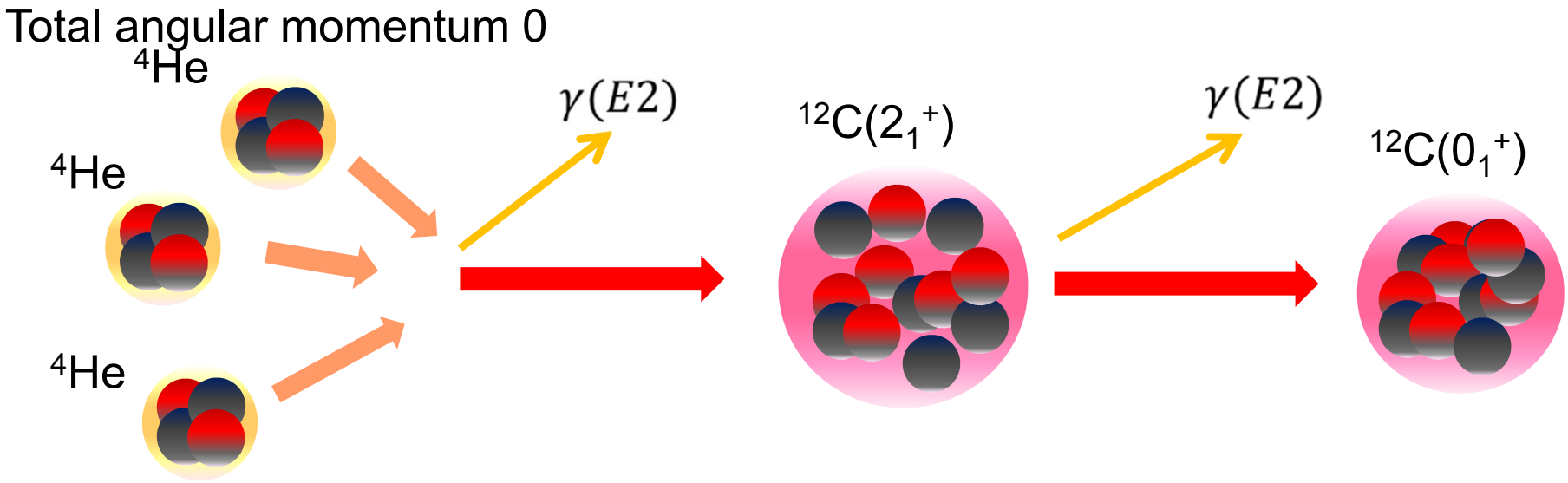

Low Temperature

Direct 3-alpha collision

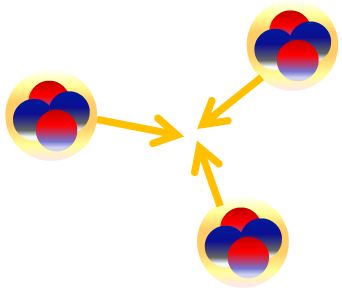

Binary collision (^{8}Be resonance)

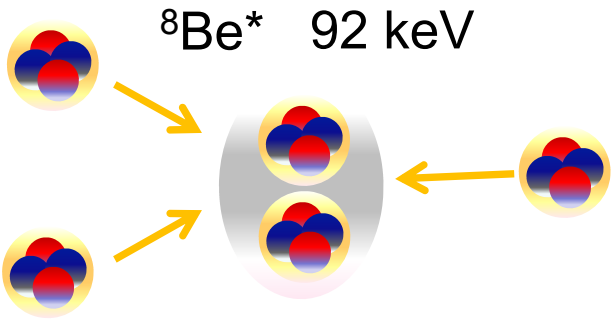

High Temperature

By way of Holy state (^{12}C resonance)

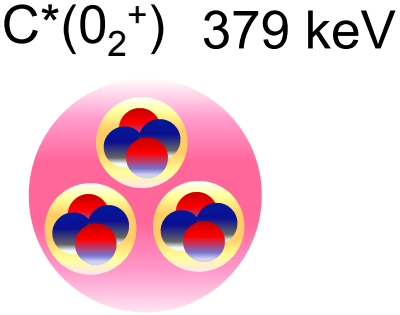

Calculated rates deviates among theories at low temperature

10^{26} order of magnitude difference at 10^7 K

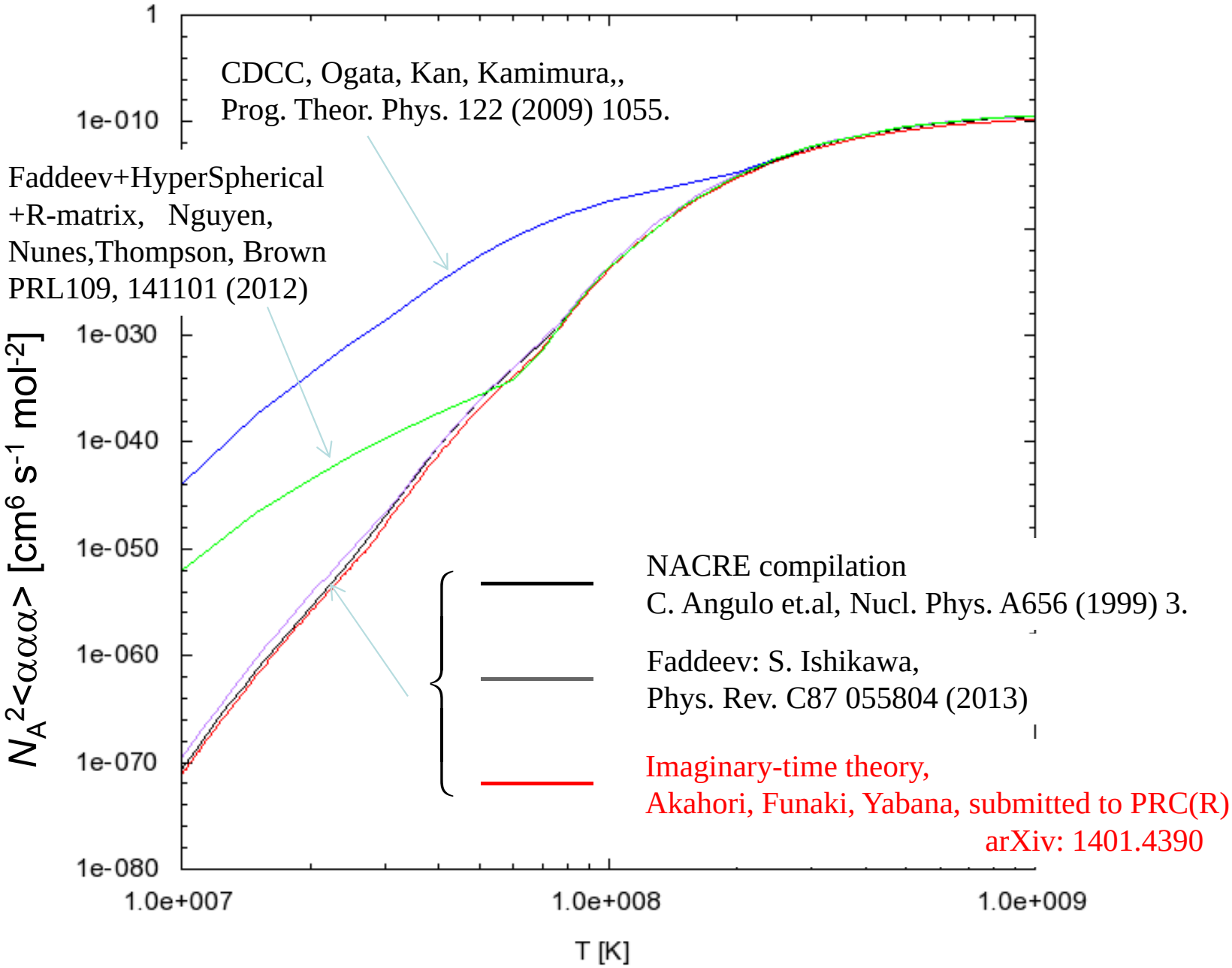

Our formulation (Imaginary-time method)

Reaction rate of $i \to f$ transition accompanying photo-emission

$$v\sigma_{fi} = \frac{8\pi(\lambda+1)}{\hbar\lambda((2\lambda+1)!!)^2}\left(\frac{E_{\vec{k}} - E_f}{\hbar c}\right)^{2\lambda+1}\left|\int d\vec{r}\,\phi_f^*(\vec{r})M_{\lambda\mu}\phi_{\vec{k}}(\vec{r})\right|^2$$

$$M_{\lambda\mu} = \sum_{i\in p} r_i^{\lambda} Y_{\lambda\mu}(\hat{r}_i)$$

λ photon multipolarity

Final: bound state

$$\int d\vec{r}\left|\phi_f(\vec{r})\right|^2 = 1$$

Initial: scattering state

$$\phi_{\vec{k}}(\vec{r}) \to e^{i\vec{k}\vec{r}} + f(\hat{r})\frac{e^{ikr}}{r}$$

Closure relation

$$1 = \sum_n \left|\phi_n\right\rangle\left\langle\phi_n\right| + \int d\vec{k}\left|\phi_{\vec{k}}\right\rangle\left\langle\phi_{\vec{k}}\right|$$

Reaction rate

$$\sum_i e^{-\beta E_i} v\sigma_{fi} \propto \int d\vec{k} e^{-\beta E_{\vec{k}}}\left(\frac{E_{\vec{k}} - E_f}{\hbar c}\right)^{2\lambda+1}\left\langle\phi_f\left|M_{\lambda\mu}\right|\phi_{\vec{k}}\right\rangle\left\langle\phi_{\vec{k}}\left|M_{\lambda\mu}{}^{+}\right|\phi_f\right\rangle$$

eliminate scattering wave function

$$= \left\langle\phi_f\left|M_{\lambda\mu}e^{-\beta\hat{H}}\left(\frac{\hat{H} - E_f}{\hbar c}\right)^{2\lambda+1}\hat{P}M_{\lambda\mu}{}^{+}\right|\phi_f\right\rangle$$

bound wave function after photo-emission

Imaginary-time evolution operator

$$\hat{P} = 1 - \sum_n \left|\phi_n\right\rangle\left\langle\phi_n\right|$$

Projector to remove bound states.

$$\beta = \frac{1}{kT}$$

Basic expression for the reaction rate in the imaginary-time theory

$$\sum_i e^{-\beta E_i} VT_{fi} \propto \left\langle \phi_f \left| M_{\lambda\mu} e^{-\beta\hat{H}} \left(\frac{\hat{H} + |E_f|}{\hbar c} \right)^{2\lambda+1} \hat{P} M_{\lambda\mu}{}^{+} \right| \phi_f \right\rangle \qquad \hat{P} = 1 - \sum_n |\phi_n\rangle\langle\phi_n|$$

Imaginary-time algorithm for practical computations

1. Prepare initial wave function

$$\psi(\vec{r}, \beta = 0) = \left(\frac{\hat{H} + |E_f|}{\hbar c} \right)^{2\lambda+1} \hat{P} M_{\lambda\mu}{}^{+} \phi_f(\vec{r})$$

2. Solve imaginary time equation

$$-\frac{\partial}{\partial\beta}\psi(\vec{r}, \beta) = H\psi(\vec{r}, \beta)$$

3. Take overlap to obtain reaction rate

$$r(\beta) \propto \int d\vec{r}\, \phi_f{}^{*}(\vec{r}) M_{\lambda\mu} \psi(\vec{r}, \beta)$$

Taylor expansion method

$$\psi(\vec{r}, \beta + \Delta\beta) = \hat{P} e^{-\Delta\beta H} \psi(\vec{r}, \beta)$$

$$\approx \hat{P} \sum_k \frac{(-\beta)^k}{k!} H^k \psi(\vec{r}, \beta)$$

- No need to solve scattering problem.
  (No boundary condition required)

- Solving in finite space amounts to bound state approximation.

K.Yabana and Y.Funaki. PRC85,055803(2012)

Convergence with respect to spatial size ($R_{\max}$ and $r_{\max}$)

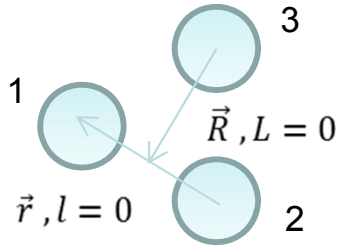

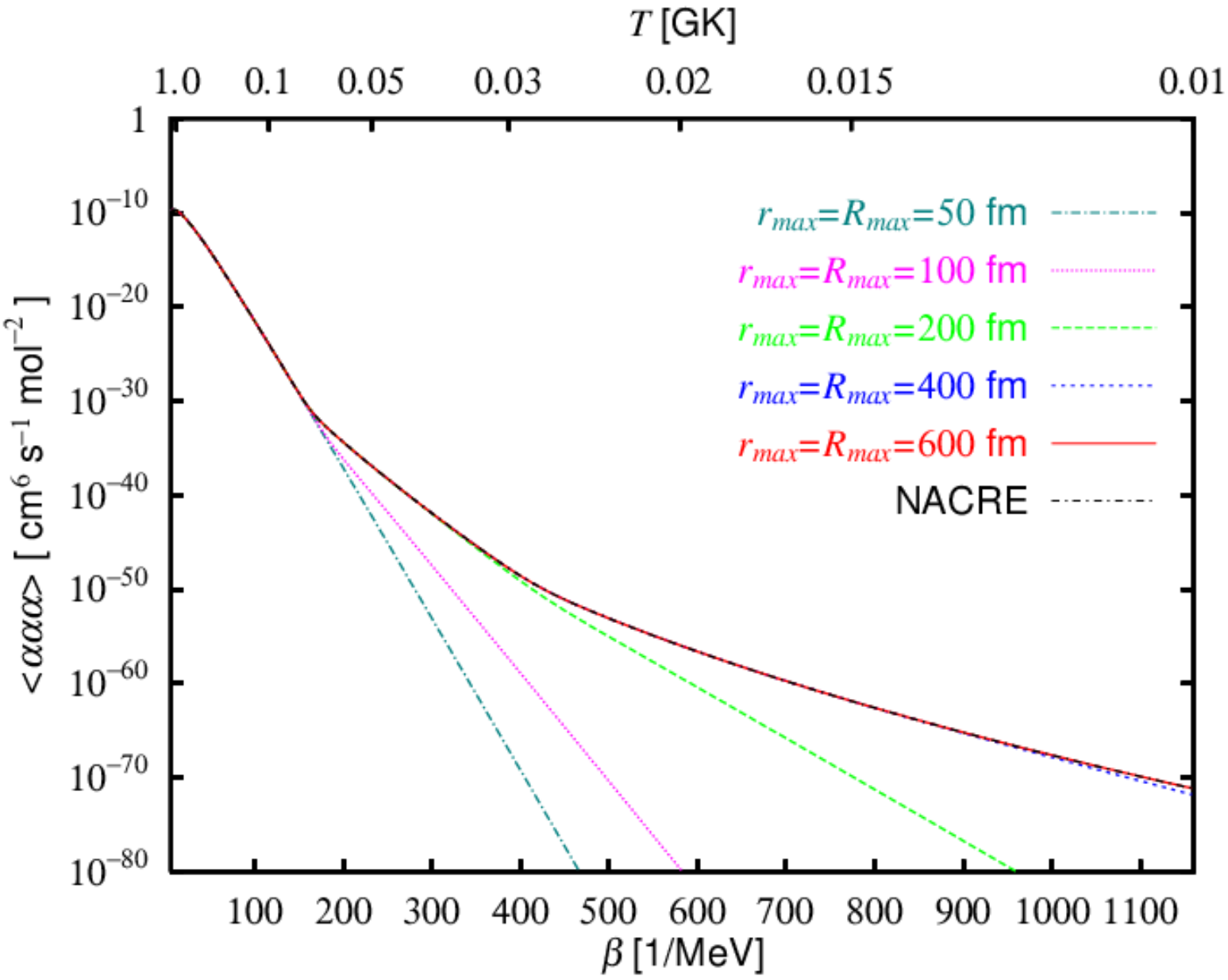

Why does CDCC give extremely large reaction rate at low temperature ?

Demonstrated by expanding our imaginary-time w.f. w.r.t. ^{8}Be+alpha

N_{max}=1 (single channel): overestimate by 10^{15}
N_{max}=400 ($E_{\alpha\alpha}$=45.4 MeV): still overestimate by 10^{12}
N_{max}=1200 (all channels) coincides with result without channel expansion.

Very slow convergence with respect to increase of channel number.

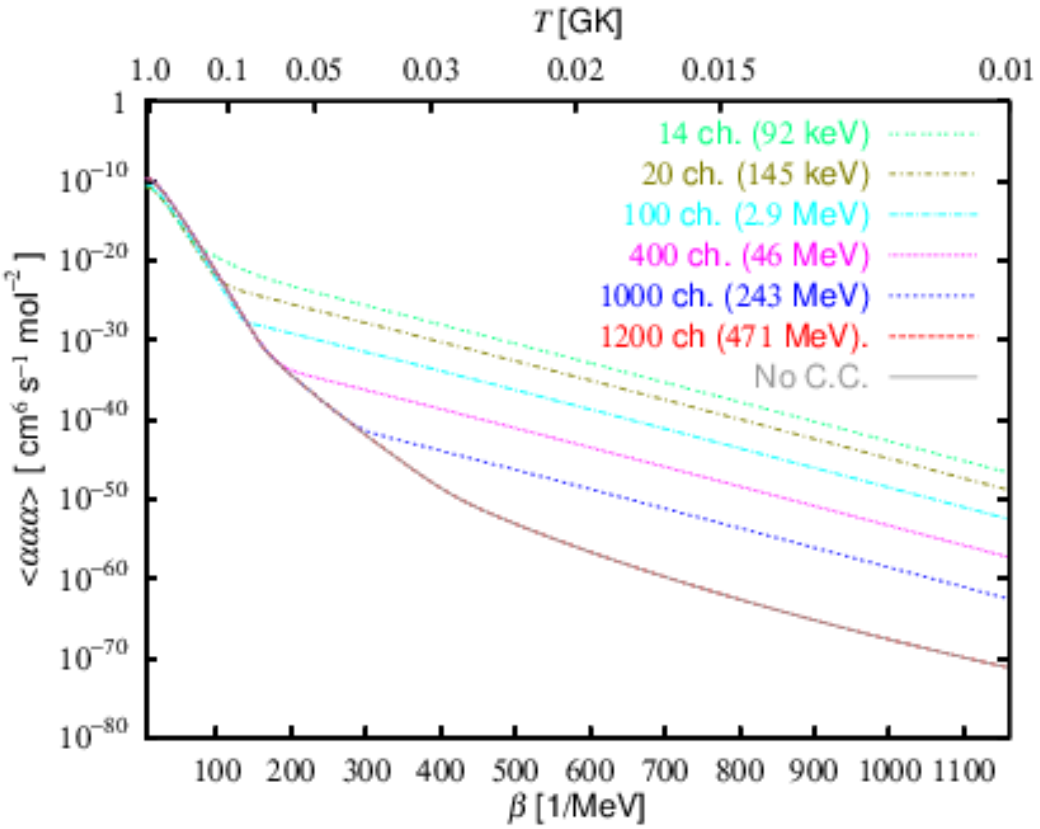

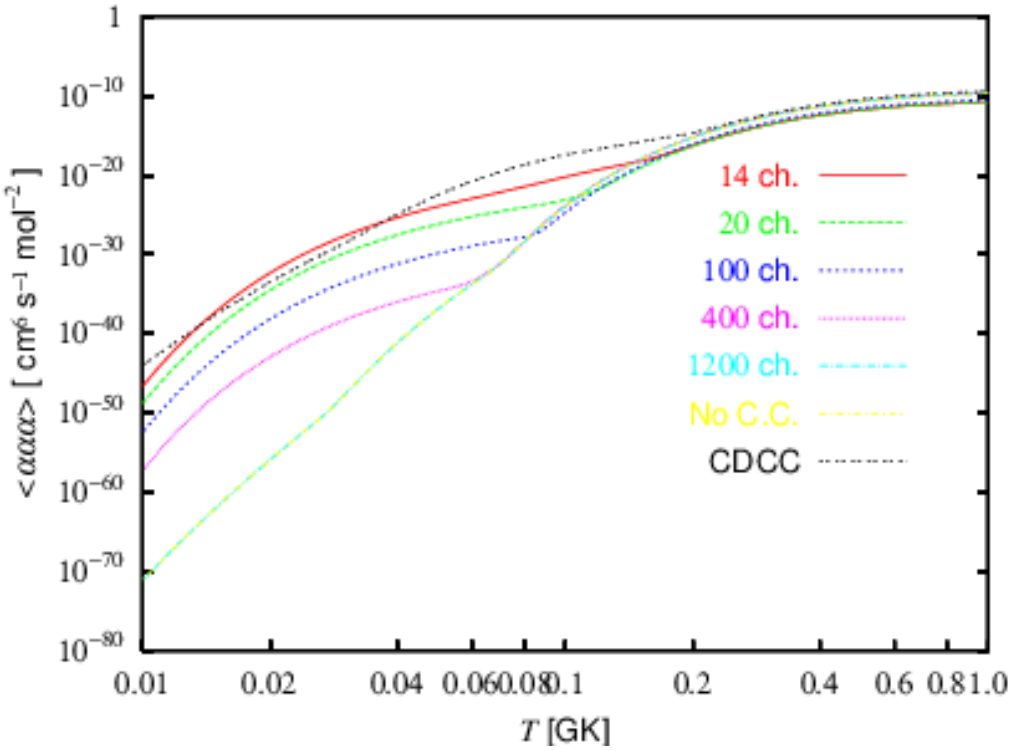

CDCC : 176 keV (122 ch.)

Summary

By using the extended version of the THSR w.f.,. based on the fact that the THSR w.f. nicely reproduces the Hoyle state.

^{12}C : 0_2^+ , 2_2^+ , 4_2^+ , 0_3^+ , 2_3^+ , 4_3^+ , 0_4^+ , 2_4^+ , 4_4^+ wave functions can be obtained.

$0_2^+ 2_2^+ 4_2^+$: large ^8Be+α components -> ^8Be+α rotational picture (however, not a simple rotation: kink in the J(J+1) line, due to the specificity of the Hoyle state (alpha condensate))

$0_3^+ 2_3^+ 4_3^+$: higher nodal ^8Be+αrotational band

$0_4^+ 2_4^+ 4_4^+$: apparently large $^8Be(2)$+α(D) components,
possibly…, 2alphas jump into D-orbit, coupling to J=0,2,4 triplets.

Rich alpha cluster dynamics built on the Hoyle state,
as if the Hoyle state were the g.s. of cluster excitations.

We have developed the imaginary-time theory for the radiative capture reaction rate.

The calculated triple-alpha reaction rate accurately coincides with that of NACRE

Truncation in the coupled-channel method gives larger reaction rate at low temperature.

Thanks

to my Collaborators

Bo Zhou (Nanjing U.)

Zhongzhou Ren (Nanjing U.)

Chang Xu (Nanjing U.)

Taiichi Yamada (Kanto Gakuin U.)

Hisashi Horiuchi (RCNP)

Akihiro Tohsaki (RCNP)

Peter Schuck (IPN, Orsay)

Gerd Röpke (Rostock U.)

Emiko Hiyama (RIKEN)

Kiyomi Ikeda (RIKEN)

Kazuhiro Yabana (U. of Tsukuba)

Takahiko Akahori (U. of Tsukuba

→ Hitachi)

and for your attention.

Why the single channel calculation so much overestimates the reaction rate?

$$\left[-\frac{\hbar^2}{2\mu}\frac{\partial^2}{\partial r^2}+v_{\alpha\alpha}(r)\right]w_n(r)=\varepsilon_n w_n(r)$$

$$\int_0^{r_{\max}} dr\, w_m(r)w_n(r)=\delta_{mn}$$

$$\sum_{n=1}\left|w_n\right\rangle\left\langle w_n\right|=1 \quad\Rightarrow\quad \left|w_{n=1}\right\rangle\left\langle w_{n=1}\right|=1$$

2α wave function (w_n(r))

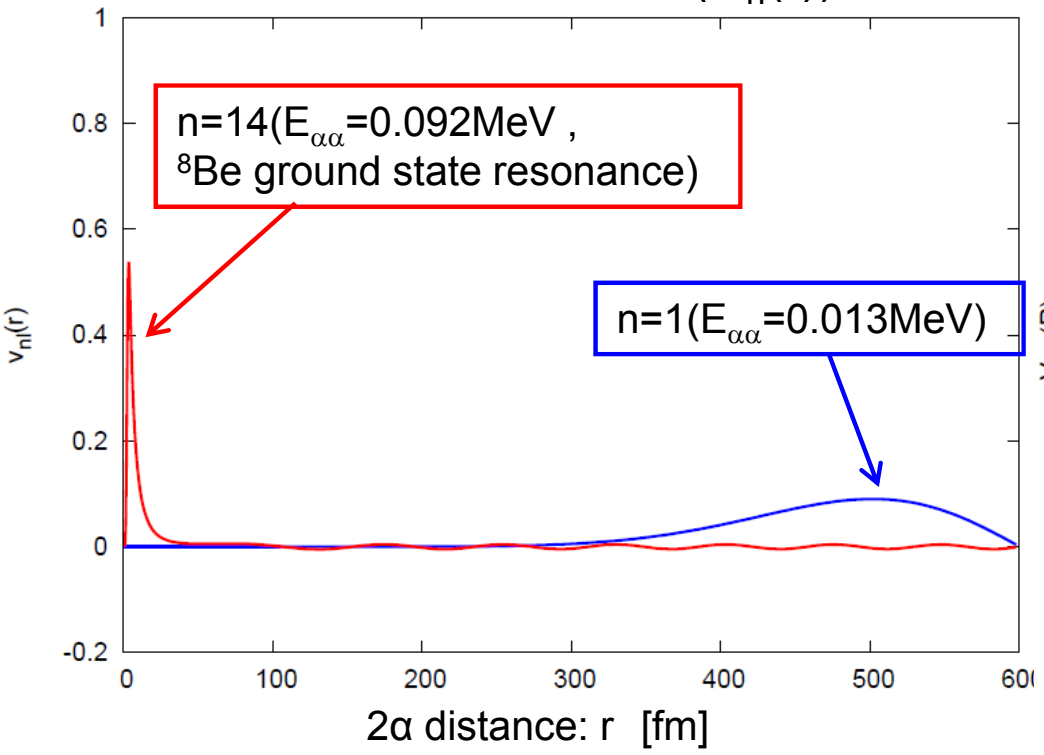

Diagonal (folding) potential (V_{nn}(R))

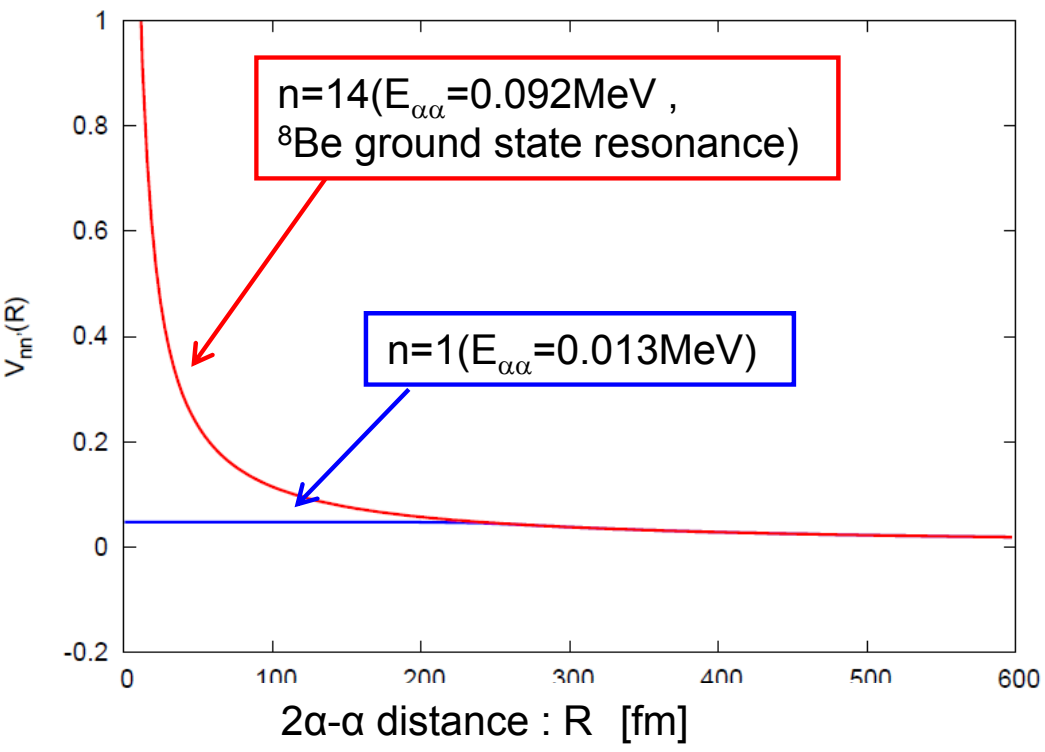

Most wave functions localize outside the Coulomb barrier.

Very small barrier for n=n'=1 channel.

Coulomb barrier for "Channel-1"

$$\sum_{n=1} |w_n\rangle\langle w_n| = 1 \;\Rightarrow\; |w_{n=1}\rangle\langle w_{n=1}| = 1$$

Since α_1 and α_2 are far away, α_3 feels very small barrier.

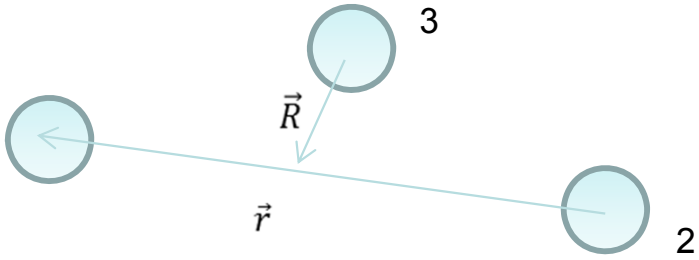

2α wave function ($v_{nl}(r)$)

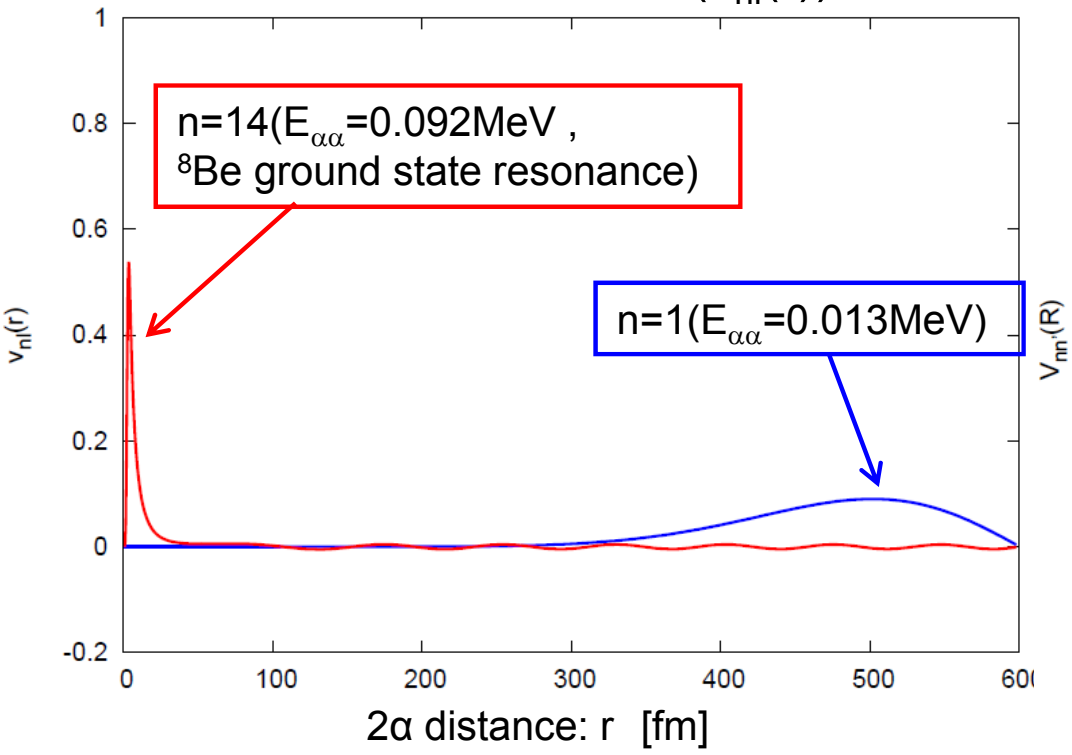

Diagonal (folding) potential ($V_{nn}(R)$)

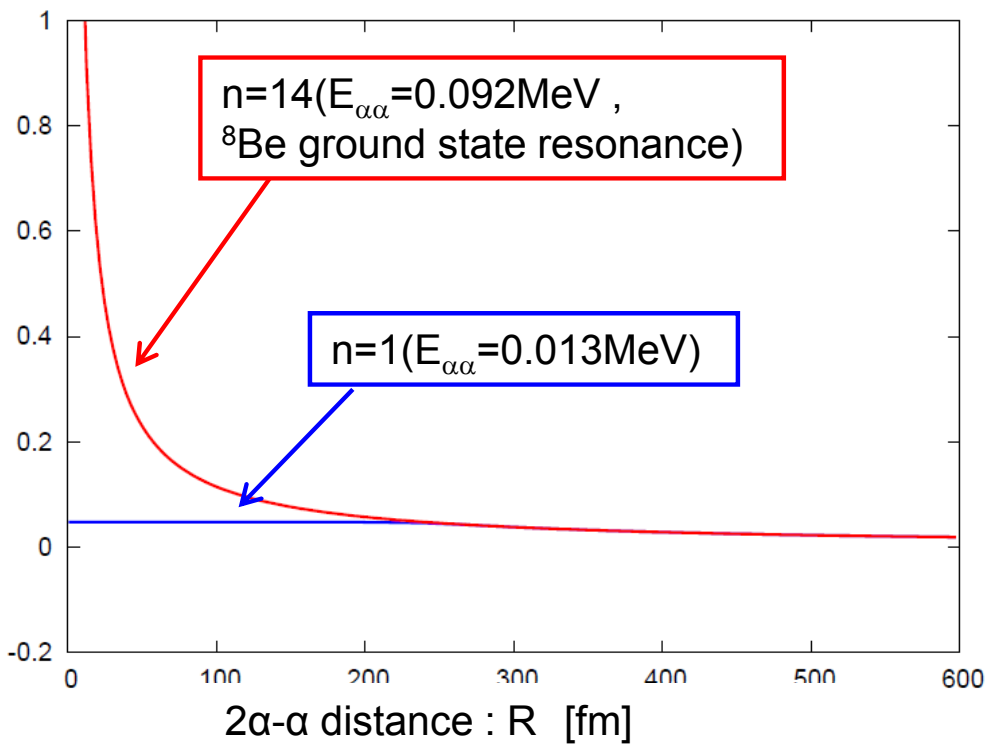

Most wave functions localize outside the Coulomb barrier.

Very small barrier for n=n'=1 channel.

Motivation and background

This, in general, gives ``container'' picture of nuclear clustering

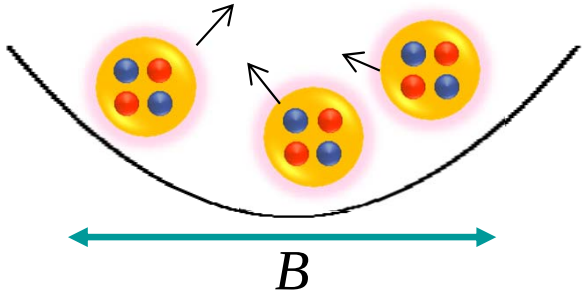

Nonlocalized clustering

Characterized by a size parameter B of the container, corresponding to nuclear size.

Where is spatial localization ?

``空間局在化''はクラスター構造の基本

H. Horiuchi, K. Ikeda, Y. Suzuki, PTPS 52, 89 (1972).

Essential in reproducing $\alpha + {}^{16}O$ inversion doublet bands.

Providing basic understanding of the nuclear clustering

Y. F. H. Horiuchi, A. Tohsaki, PPNP82, 78-132 (2015).

Motivation and background

This, in general, gives ``container'' picture of nuclear clustering

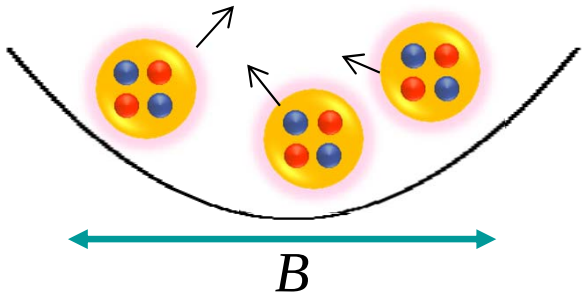

Nonlocalized clustering

Characterized by a size parameter B of the container, corresponding to nuclear size.

Where is spatial localization ?

``空間局在化''はクラスター構造の基本

H. Horiuchi, K. Ikeda, Y. Suzuki, PTPS 52, 89 (1972).

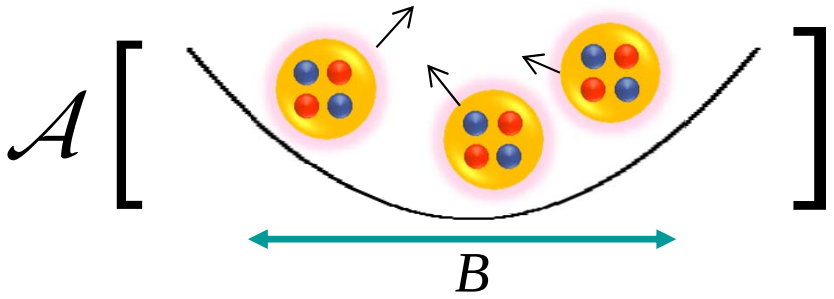

Essential in reproducing $\alpha + {}^{16}\mathrm{O}$ inversion doublet bands.

Providing basic understanding of the nuclear clustering

Y. F. H. Horiuchi, A. Tohsaki, PPNP82, 78-132 (2015).

Motivation and background

This, in general, gives ``container'' picture of nuclear clustering

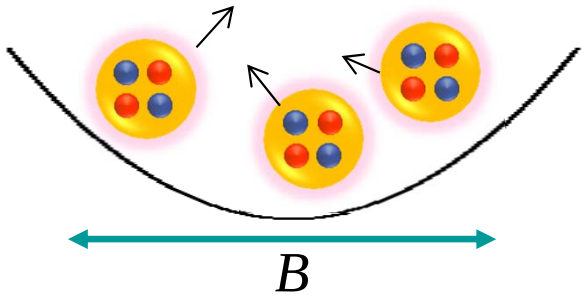

Nonlocalized clustering

Characterized by a size parameter B of the container, corresponding to nuclear size.

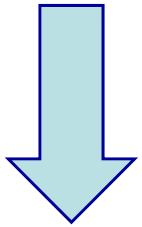

``The core-like repulsion is attributed to the strong exchange kernels due to the Pauli principle and less repulsive as L goes larger; …''

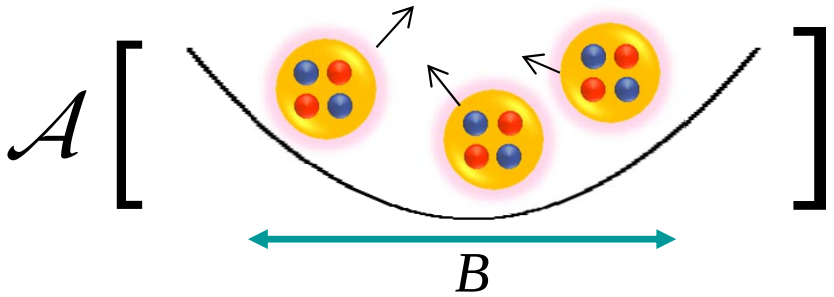

J. Hiura and R. Tamagaki, PTPS52, 25 (1972).

I. Shimodaya, R. Tamagaki, H. Tanaka, PTP 27, 793 (1962).

Spatial localization: coming from antisymmetrization

Providing basic understanding of the nuclear clustering

Y. F. H. Horiuchi, A. Tohsaki, PPNP82, 78-132 (2015).

Imaginary-time method (3/3): Computational procedure

Basic expression for the reaction rate in the imaginary-time theory

$$\sum_i e^{-\beta E_i} VT_{fi} \propto \left\langle \phi_f \left| M_{\lambda\mu} e^{-\beta\hat{H}} \left(\frac{\hat{H} + |E_f|}{\hbar c} \right)^{2\lambda+1} \hat{P} M_{\lambda\mu}{}^{+} \right| \phi_f \right\rangle \qquad \hat{P} = 1 - \sum_n |\phi_n\rangle\langle\phi_n|$$

Imaginary-time algorithm for practical computations

1. Prepare initial wave function

$$\psi(\vec{r}, \beta = 0) = \left(\frac{\hat{H} + |E_f|}{\hbar c} \right)^{2\lambda+1} \hat{P} M_{\lambda\mu}{}^{+} \phi_f(\vec{r})$$

2. Solve imaginary time equation

$$-\frac{\partial}{\partial\beta}\psi(\vec{r}, \beta) = H\psi(\vec{r}, \beta)$$

3. Take overlap to obtain reaction rate

$$r(\beta) \propto \int d\vec{r}\, \phi_f{}^{*}(\vec{r}) M_{\lambda\mu} \psi(\vec{r}, \beta)$$

Taylor expansion method

$$\psi(\vec{r}, \beta + \Delta\beta) = \hat{P} e^{-\Delta\beta H} \psi(\vec{r}, \beta)$$

$$\approx \hat{P} \sum_k \frac{(-\beta)^k}{k!} H^k \psi(\vec{r}, \beta)$$

- No need to solve scattering problem.
  (No boundary condition required)

- Solving in finite space amounts to bound state approximation.

K.Yabana and Y.Funaki. PRC85,055803(2012)